Constructing the holographic realization of a Luttinger Liquid/ Low dimensional AdS/CMT

Master thesis by
Mathijs Janssen

Supervised by
Andrei Parnachev and Jan Zaanen

July 28, 2012

Acknowledgements

This had been quite a year for me. It is strange how a decision you make in a few days, based on little knowledge, will shape the rest of your year. Not aware of the fact that my home university in Utrecht was also starting up in AdS/CMT but intrigued by this fascinating area I decided to go to the place which already had a (relatively) long record in this new exciting field. My unconventional move to Leiden to write my master thesis, combined with my stubborn unwillingness to travel five days a week resulted in a year where I spent more time in the university libraries than anywhere else. Once a week I travelled to Leiden, which turned out to be a warm nest where I met inspiring people from all over the world.
Working at the same university where Heike Kamerlingh Onnes discovered superconductivity in 1911 was special, not in the least because application of the AdS/CFT correspondence to condensed matter, the subject of this thesis, might shed light on the ill-understood phenomenon of high-temperature superconductivity. In the same tradition as Ehrenfest who invited the top of physicists of his days to Leiden, I was able to meet inspiring professors like Johanna Erdmenger and Subir Sachdev, the Lorentz Professor of 2012.

First of all my biggest thanks are to Andrei who patiently helped me with my problems and with whom I had countless stimulating discussions. I thank Jan for selflessly accepting me as his master student even though there might not have been any benefit for Leiden University. I am thankful also for all the interesting conservations we had about topics ranging from (besides physics): entrepreneurship, microcredit in the third world, German cars, addiction, attraction, Uzbekistan and so forth. I thank Mihailo for the help with the numerical simulations and discussions in general.

I thank; Cristiane de Morais Smith for introducing me to the people in Leiden,
Subir Sachdev for pointing out the route of section 6.3, which he sketched on the board after my presentation in Leiden,
Kostas Skenderis for allowing me to join the Holographic Fluids workshop organized at the UvA in January,
Juan Jottar for allowing me to join the String Theory workshop at the UvA, where I was able to attend lectures and talk to leading figures in the field such as Sean Hartnoll, John McGreevy and David Tong.
Thanks to Hong Liu for answering my emails.

I thank Peter and Watse for comments on my draft, and Watse also for the liters of coffee he donated to me during our many discussions in the library,
my parents for their unconditional love, understanding, appreciation and financial support.

Conventions and Notation

Units in which $c = \hbar = 1$ are used. A spacetime of dimensionality $D = d + 1$ has d spatial dimensions, e.g. in a spacetime with (t, x, y, z), $D = 4$ and $d = 3$. The metric has a mostly plus $(-, +, +, ...)$ signature. Four-vectors are denoted by $k = (\omega, \mathbf{k})$, that is, bold face quantities are spatial vectors.

Often occuring symbols are:

L	curvature radius of AdS (put to $L = 1$ mostly)
G_N	Newton's constant in N dimensions
κ	related to Newton's constant via $\kappa^2 = 8\pi G_N$
g_f	effective dimensionless gauge coupling
q	charge of fermion field ψ
r	radial coordinate to parametrize AdS. Takes values between $r = \infty$ at the AdS-boundary and $r = 0$ in the deep interior of AdS
r_h	location of black hole horizon (put to $r_h = 1$ mostly)
L_2	curvature radius of near horizon $\mathrm{AdS}_2 \times \mathbb{R}$ geometry, $L_2 = \frac{1}{\sqrt{2}} L = \frac{1}{\sqrt{2}}$
ζ	near horizon radial coordinate; $\zeta = \frac{L_2^2}{r - r_h}$
Q	black hole charge
$D(i\Omega, k, r, r')$	fermionic bulk-to-bulk propagator
$\mathcal{G}_k(\Omega)$	IR retarded Green's function of the $\mathrm{AdS}_2 \times \mathbb{R}$ boundary.
$G_R(\Omega, k)$	boundary retarded Green's function

Contents

1 Introduction **1**

2 Luttinger liquid theory **5**

2.1 Fermi liquid theory 6

2.2 The breakdown of Fermi liquid theory in low dimensions 7

2.3 Luttinger model 9

2.3.1 Bosonization 10

2.3.2 Exact density-density correlation function 12

3 AdS/CFT and its application to condensed matter **15**

3.1 Indications towards AdS/CFT 15

3.2 The formulation 16

3.3 Connection to condensed matter physics 18

3.3.1 Temperature 19

3.3.2 Finite density 20

3.4 Renormalization and double trace deformations 20

3.5 Historical overview of AdS/CMT 21

4 The Charged BTZ black hole **23**

4.1 Gauge field 23

4.2 Solving Einstein's equations 25

4.3 Near horizon analysis of extremal BTZ 26

5 Fermions in a BTZ background **29**

5.1 Dirac equation and Spin connection 29

5.2 Boundary Green's function of $\mathrm{AdS}_2 \times \mathbb{R}$ 32

5.3 Boundary Green's function of full background 35

6 Quantum Corrections **37**

6.1 Construction of fermionic propagator 38

6.2 Effective vertices 41

6.2.1 Near horizon: $\zeta\omega \gg 1$ 42

6.2.2 The boundary of the near horizon $AdS_2 \times \mathbb{R}$ region: $\zeta\omega \ll 1$ 43

6.2.3 UV: bulk $AdS_3 - BTZ$ 44
6.3 Analytic results 45

7 Conclusion and Discussion **47**

A Linear Response **49**
A.1 Microscopic considerations 50
A.1.1 The plethora of real-time response function 50
A.2 The spectral function 51

B Curvature and the Einstein Equation **53**

C Bibliography **57**

Chapter 1

Introduction

BCS theory, which describes ordinary superconductivity with great success, is not sufficient to explain the high-temperature superconductivity found in cuprates. Despite great theoretical effort, a new framework to describe this phenomenon is still not found. A whole new approach, radically departing from conventional condensed matter techniques, makes use of the anti de Sitter/conformal field theory correspondence (AdS/CFT correspondence). This duality, emerging out of string theory in the end of the '90s, seems taylor made to describe strongly coupled many-body systems, such as the aforementioned cuprates. Because AdS/CFT is a weak-strong duality, complicated condensed matter problems which due to strong coupling cannot be solved with perturbative methods, can be mapped onto a theory defined on a curved background in one dimension higher, where things drastically simplify. As such, AdS/CFT is a valuable tool in the study of strongly coupled systems.
Since the correspondence is, as of yet, not proven rigorously; we will take a pragmatic standpoint, anticipate its correctness, and investigate the implications of the correspondence for low-dimensional systems. In 1+1 dimensions a theory of interacting fermions with a gapless linear dispersion is exactly solvable. Through the method of bosonization these interacting fermions can be mapped onto a theory of non-interacting bosons, where a variety of physical observables can be obtained exactly. This so called Luttinger model (for reviews see [1, 2, 3] and references therein) possesses a number of distinct features, among which spin-charge separation and anomalous scaling dimensions for correlation functions. Like Fermi liquid theory, which describes a system of weakly interacting fermions with great success in higher dimensions, the Luttinger liquid has a sharp Fermi surface. Essential to Fermi liquid theory are the existence of low-lying quasiparticles. The original particles are 'dressed' by the interactions in the sense that their original properties are replaced with renormalized values. The small phase space of the Luttinger model (the Fermi surface is made out of two points at $\pm k_f$) forbids the occurrence of quasiparticles. The only excitations of the Luttinger model are collective excitations, which have bosonic properties. Because of the absence of fermionic quasiparticles Luttinger liquids are called *non-Fermi liquids*.

We will try to reproduce and find signatures of these non-Fermi liquid features on the gravitational side of the AdS/CFT correspondence. This means that we aim for a better understanding of the AdS side of the correspondence by trying to reproduce an exactly solvable, strongly coupled field theory. To keep matters as simple as possible we will focus on a spinless Luttinger liquid. Although there will be no spin/charge

separation, the anomalous scaling of correlation functions should still hold true.

The AdS/CFT correspondence states that fields ϕ that live in the bulk couple on the boundary of AdS to operators $\mathcal{O}$ in the CFT. The GPKW equation $\langle e^{-\int \phi_0 \mathcal{O}} \rangle_{CFT_{1+1}} = \mathcal{Z}_{SUGRA}(\phi_0)$ enables one to calculate any n-point correlation function $\langle \mathcal{O}(x)...\mathcal{O}(0) \rangle$ by taking functional derivates to the fields ϕ_0 on both sides.[1] The quantity appearing on the right-hand side however can only be approximated. In the context of AdS/CFT this is done by taking a large N limit in which the supergravity partition function is approximated semi-classically by the largest Euclidean saddle of the Einstein-Hilbert action with negative cosmological constant,

$$\langle e^{-\int \phi_0 \mathcal{O}} \rangle_{CFT_{1+1}} = \mathcal{Z}_{SUGRA}(\phi_0) \approx e^{-S_{on-shell}[\phi_0]} + \mathcal{O}(1/N). \tag{1.1}$$

A solution to 2+1 dimensional gravity with a negative cosmological constant was found by Bañados, Teitelboim and Zanelli [4]. To be more specific, the BTZ metric together with a gauge potential $A_t = \rho \log r/r_h$ solve Einstein's equations which arise after variation of the Einstein-Hilbert-Maxwell action with negative cosmological constant.
The BTZ metric is asymptotically AdS_3 and via the AdS/CFT correspondence we can therefore study a dual field theory which is $1+1$ dimensional. The $U(1)$ gauge field on the gravity side maps (by the AdS/CFT dictionary) to a nonzero chemical potential μ for a $U(1)_{charge}$ i.e. a conserved current J_μ. This means that the boundary field theory obtains a finite charge density. Written in Euclidean signature the time component of the metric has a deficit angle which, after a periodic identification, is interpreted as the black hole temperature. This Hawking temperature vanishes if the inner and outer BTZ horizons merge, which is the case if the black hole is extremely charged. As was found in [5] for higher-dimensional AdS black holes, and proven for the low-dimensional BTZ in section 4.3, this leads to a $AdS_2 \times \mathbb{R}$ near horizon geometry. The AdS_2 part of this metric hints in the direction that this metric has *emergent conformal symmetry* in the near horizon area (an observation on which I will elaborate in chapter 4).

Generalizing Birkhoff's theorem we show in section 4.2 that the charged BTZ is the unique static, spherically symmetric solution to low-dimensional gravity with negative curvature and a non-zero electric field on the asymptotic boundary.
We pose the configuration "BTZ + matter fields" as a good candidate to holographically describe a Luttinger liquid.

The hypothesis formulated above does not apply the other way around. It might happen that in some range of parameters in the AdS bulk, a field theory is produced on the boundary that is not a Luttinger liquid. This means that the boundary field theory is not described by a theory of interacting fermions *solely* and new additional (gauge) fields need to be introduced on the boundary.

As stated before, we will try to find the signatures of Luttinger liquids also on the bulk side of AdS/CFT. One of the correlation functions in Luttinger liquid theory which shows anomalous scaling is the density-density correlation function. This real space correlation function has a $2k_f$ part which decays with a power

[1] The notation $\lim_{r\to\infty} \phi(r) \equiv \phi_0$ is used.

depending on the interaction couplings (see 2.28).
The charge density ρ is the $t-$component of the four-current J_μ which, via the AdS/CFT correspondence, couples to the asymptotic value of the gauge field A_μ that lives in the bulk. Finding the density two-point function therefore comes down to finding the tt-component of the gauge field propagator.

It was found by several authors that the large N result does not display any of the aforementioned interesting $2k_f$ singularities [6][7]. The claim we make is that this must be an artifact of the large N limit. Put differently, we conjecture (logarithmic-divergent) quantum corrections which arise at finite N to be responsible for the anomalous scaling dimension.[2] Another possibility to include corrections is by adding higher derivative terms to the Einstein-Hilbert action. This is a tricky procedure, in general associated with ghosts, on which we will not elaborate in this thesis.

Matter is added to the BTZ spacetime in the form of a fermionic field ψ of mass m_ψ and charge q (see 5.2). Working in the so-called probe limit, the fields will not back-react on the metric. The coupling of the gauge field to the fermions in the action gives rise to the one loop diagram depicted in figure 6 (page 37). This quantum loop correction in the bulk is 1/N suppressed and thereby allows us to obtain results away from the large N limit. Note however that diagrams in the bulk do not need to have a clear connection to a counterpart (scattering) process on the boundary. A fermionic loop correction to a gauge field in the bulk is therefore not necessarily equivalent to the same process occurring in the field theory.
To make this statement more acceptable, consider the stress-energy tensor $T_{\mu\nu}$ of the field theory which, via the AdS/CFT dictionary, couples to the metric $g_{\mu\nu}$ on the AdS boundary. In order to calculate corrections to this $T_{\mu\nu}$ using AdS/CFT one would consider graviton scattering processes on the bulk side. This clearly does not have any counterpart interpretation in the CFT.
The interesting observation we make is that, the above considerations put aside, the bubble diagram in the BTZ background *will* to a large extent resemble the calculation of the density two point function in field theory. To find this we need to group all the radial dependent terms of the loop amplitude into *effective vertices*.

Also in higher dimensions quantum corrections can be of value. This work will be very much in the spirit of some recent papers which tried to capture physical phenomena including 't Haas van Alphen oscillations [8] [9] and the Coleman-Mermin-Wagner theorem [10] which are not visible in the large N limit.[3]

This thesis is organized as follows; in chapter 2 the theory of Fermi liquids and Luttinger liquids is reviewed. This is more or less textbook material so we will be brief at some places, referring the reader to references where necessary. To come to a holographic description of low-dimensional fermion systems, first the basic principles of the AdS/CFT correspondence must be touched upon, which will be the topic of chapter 3. Being the unique black hole solution to the Einstein equation with negative curvature, the BTZ black hole is presented (chapter 4) as the best candidate to start this holographic computation. In chapter 5 we introduce fermions in the BTZ background and analyze the Dirac equation for various regions

[2] In the large N limit quantum corrections on the bulk side are suppressed with a factor $\frac{L^{d-1}}{G_N} \sim N \gg 1$.

[3] Compare this to the old result of Witten [11]. He showed that in the $SU(N)$ Thirring model, the large N-limit suppresses the infrared fluctuations that wash out expectation values. Moving away from large N correctly produces the algebraic long range order that is to be expected due to Coleman's theorem (no spontaneous breaking of continuous symmetry in low dimensional systems).

of spacetime. In chapter 6 we move away from the large N limit to investigate whether the anomalous scaling dimensions, which are a non-mean field phenomenon, present themselves when quantum corrections are performed. This is done by calculating the loop correction to the gauge field two-point function. This thesis is concluded with a discussion in chapter 7.

With Blaise Pascal in the back of my mind ("Je n'ai fait celle-ci plus longue parceque je n'ai pas eu le loisir de la faire plus courte") I decided not to include the calculation I spent most time on: the loop correction to the scalar propagator. In retrospect this calculation had little physical relevance and would have added twenty pages with the same procedure as outlined in the last three chapters, but with different details.

Chapter 2

Luttinger liquid theory

Systems of interacting electrons are almost always very well described by Fermi liquid theory. There are however two important exceptions; the first is when interactions become exceedingly large (interaction energy due to Coulomb force stronger than kinetic energy), the second is when the electrons confined in a space of low dimensionality.
This chapter will argue why one dimensional electron systems show behavior that is distinct from electrons in higher dimensions. On an intuitive level this is clear from the observation that an electron moving in one dimension has no room to avoid other electrons. Even for weak interactions the electrons are therefore strongly coupled. Any individual motion has to becomes collective. Because the only low-lying excitations are collective excitations, which have bosonic properties, a description in terms of a fermionic quasiparticle is not possible.

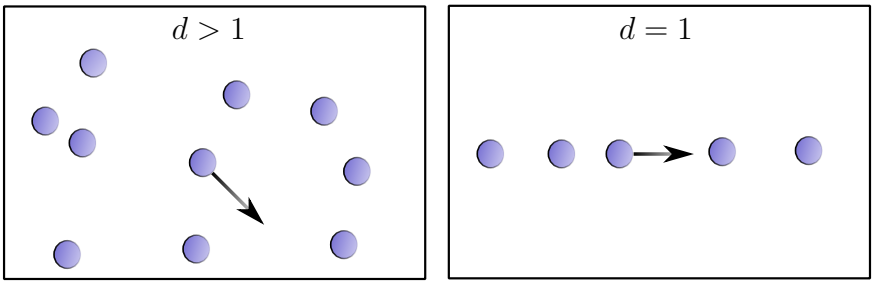

Figure 2.1: Electrons moving in d dimensions. The degree to which particles can move freely depends not only on the strength of the interactions but also on the dimensionality of the system.

Before we embark on our one dimensional journey it is wise to first review Fermi liquid theory, this is done in section 2.1. The breakdown of Fermi liquid theory in low (1+1) dimensions can then be concretized in section 2.2. In the final section 2.3 the Luttinger model is introduced, whose generalization, the Luttinger liquid, is believed to capture the dynamics of interacting electrons confined in one dimension. The absence of a quasiparticle led people to call this theory a *non-Fermi Liquid*.

2.1 Fermi liquid theory

Landau-Fermi liquid theory is the generalization of the Fermi gas, non-interacting fermions, to a system of interacting fermions. The theory, developed by Landau (see: [12] [13] [14]), has been so successfull that usually Landau's name is omitted and interacting fermions are said to be described by Fermi liquid theory. In the Fermi gas, the Pauli exclusion principle prohibits fermions to all be in the lowest momentum state. As a result a Fermi sea is formed, filling up level by level up to a Fermi energy ϵ_f. The occupation number $n(\epsilon)$ at $T = 0$ is given by $n(\epsilon) = \Theta(\epsilon_f - \epsilon)$; where Θ is the Heaviside step function. It has a discontinuity of height 1 at k_f. The excitations of the non-interacting Fermi gas have a well-defined energy and momentum. Particles can be created with momentum $|\vec{k}| > k_f$ and they have energy $\epsilon_k = \epsilon - \mu > 0$. Also holes can be created within the Fermi sea and they have momentum $|\vec{k}| < k_f$ and energy $\epsilon_k = \mu - \epsilon > 0$. These excitations have an infinite lifetime because they are eigenstates of the Hamiltonian. This is reflected by a spectral function with delta function peak at the particle energy (see equation A.14).

In principle interacting fermions are hard to describe because, in typical conductors, the energy due to Coulomb interactions is of the same order of magnitude as the kinetic energy of the particles. Put differently, interaction energies do not dominate nor do they vanish.[1] This seems not to be a favorable position to start a perturbation theory. Landau found a way however to describe these systems which is very powerful because it works even for interactions which are not small.
Starting in a non-interacting system and switching on the interactions *adiabatically*, the fundamental particles with which Landau's theory describes the system are no longer the bare electrons, but electrons 'dressed with density fluctuations'. These new particles are called *quasiparticles*. They are either non-interacting, or interactions are at least controllable. Quasiparticles have the same quantum numbers as the constituent particles, their mass however and also dynamical properties (e.g. specific heat, susceptibility) obtain renormalized values. The quasiparticles have a finite lifetime τ, which manifests itself as a nonzero self-energy in the single-fermion Green's function at $k - k_f \approx 0$,

$$G_R(\omega, k) = \frac{Z}{\omega - v_f k + i\omega^2}, \tag{2.1}$$

leading to a Lorentzian profile in the spectral function (see equation A.15). The lifetime (width of the Lorentzian $1/\tau$) diverges as $\tau \sim (E - E_f)^2$ when the energy approaches the Fermi energy. The quasiparticles can therefore be considered approximately stable because in real metals the Fermi energy is very large compared to excitation energies, $E_f \sim 3eV$ or $T_f = \frac{E_f}{k_b} \sim 10000K$.
The factor Z appearing in 2.1 reflects the fact that, due to the interactions, the occupation number $n(\epsilon)$ of the Fermi liquid is not a Heaviside step function any more but the height decreases from 1 to $Z = \left(1 - \frac{\partial \Sigma'}{\partial \omega}\right)^{-1}$, where Σ' is the real part of the self-energy.
A renormalization proof of Landau's theory of Fermi liquids was given by [15] [16]. Being a free stable RG fixed point underlines the robustness of the theory and the quasiparticles is relies upon.

[1] The lowest kinetic energy an electron can have follows from the uncertainty principle $E_{kin} = \frac{\hbar p^2}{2m} \sim \frac{\hbar}{mr^2}$. The energy due to Coulomb forces between nearest neighbor electrons scales as $\frac{e^2}{r}$. Dividing the two gives an dimensionless ratio which is denoted by r_s. This r_s is the radius of a sphere that on average contains one electron. For typical metals $r_s \sim 1$.

2.2 The breakdown of Fermi liquid theory in low dimensions

The formalism reviewed in the appendix A puts us in a position where we can see why Fermi liquid theory cannot describe fermions in one spatial dimension. The concept of adiabatic continuity does not apply for fermions in one dimension. This is because switching on an *infinitesimal* interaction between the particles already drastically changes the behavior of the system.
Doing perturbation theory in this interaction, terms will appear containing the density-density correlation function. In this subsection I will show that the full density susceptibility, in the random phase approximation (RPA), diverges at a special vector called the *nesting vector*. This divergence signals an instability towards the formation of an ordered phase, which in low dimensions, due to Mermin-Wagner, cannot happen.
To that end, consider the density susceptibility (the Fourier transform of the density-density correlation function)

$$\chi(\vec{q}, i\omega) = -\int_0^\beta d\tau e^{i\omega_n \tau} \langle T_\tau \rho(\vec{q}, \tau)\rho(-\vec{q}, 0)\rangle. \tag{2.2}$$

Now using that the density operator $\rho(x) = \hat{c}_x^\dagger \hat{c}_x$, which destroys and creates a particle at location x, in momentum space is $\rho(q) = \sum_k \hat{c}_{k+q}^\dagger \hat{c}_k$,[2]

$$\begin{aligned}
\chi(\vec{q}, i\omega) &= -\sum_{k,k'} \int_0^\beta d\tau e^{i\omega_n \tau} \langle T_\tau \hat{c}_{k+q}^\dagger(\tau)\hat{c}_k(\tau)\hat{c}_{k'-q}^\dagger(0)\hat{c}_{k'}(0)\rangle \\
&= -\sum_{k,k'} \int_0^\beta d\tau e^{i\omega_n \tau} \Big[\langle T_\tau \hat{c}_{k+q}^\dagger(\tau)\hat{c}_k(\tau)\rangle\langle T_\tau \hat{c}_{k'-q}^\dagger(0)\hat{c}_{k'}(0)\rangle - \langle T_\tau \hat{c}_{k+q}^\dagger(\tau)\hat{c}_{k'}(0)\rangle\langle T_\tau \hat{c}_{k'-q}^\dagger(0)\hat{c}_k(\tau)\rangle\Big] \\
&= -\sum_{k,k'} \int_0^\beta d\tau e^{i\omega_n \tau} \Big[\cancel{\delta_{k+q,k}\mathcal{G}(k+q,0)\delta_{k'-q,k'}\mathcal{G}(k'-q,0)} - \delta_{k+q,k'}\mathcal{G}(k+q,\tau)\delta_{k'-q,k}\mathcal{G}(k'-q,-\tau)\Big] \\
&= \sum_k \int_0^\beta d\tau e^{i\omega_n \tau} \mathcal{G}(k+q,\tau)\mathcal{G}(k,-\tau).
\end{aligned} \tag{2.3}$$

The negative τ component in the third line, a particle traveling backward in imaginary time, is interpreted as a hole traveling forward in imaginary time. The density susceptibility is therefore a sum over the momentum exchange in particle-hole bubbles.

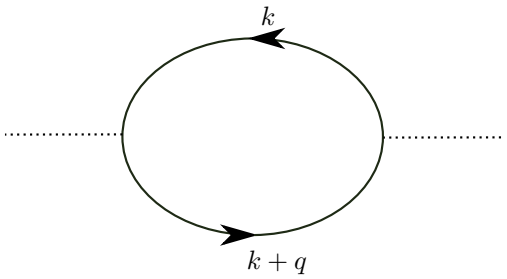

Figure 2.2: Particle-hole bubble contributing to the density-density susceptibility.

[2]This simply follows after Fourier decomposition $\rho(x) = \sum_{k,k'} \frac{1}{\Omega} e^{i(k-k')x} \hat{c}_{k'}^\dagger \hat{c}_k \equiv \sum_q \frac{1}{\Omega} e^{iqx} \rho(q)$.

The above expression is cast into a more useful form,

$$\begin{aligned}\chi(\vec{q},i\omega) &= \sum_k \sum_{l,m} \int_0^\beta d\tau e^{i\omega_n\tau}\mathcal{G}(k+q,i\omega_l)e^{-i\omega_l\tau}\mathcal{G}(k,i\omega_m)e^{i\omega_m\tau} \\ &= \sum_k \sum_{l,m} \int_0^\beta d\tau \mathcal{G}(k+q,i\omega_l)\mathcal{G}(k,i\omega_m)e^{i\tau(\omega_n-\omega_l+\omega_m)} \\ &= \sum_k \sum_m \mathcal{G}(k+q,i\omega_{m+n})\mathcal{G}(k,i\omega_m). \end{aligned} \tag{2.4}$$

In the case of a free Fermi gas this sum can be evaluated by inserting the single-particle propagator,

$$\begin{aligned}\chi(\vec{q},i\omega) &= \frac{2T}{L^3}\sum_k \frac{1}{-i\omega_{m+n}+\xi_{\mathbf{k+q}}}\frac{1}{-i\omega_m+\xi_{\mathbf{k}}} \\ &= \frac{2T}{L^3}\sum_{\mathbf{k}}\sum_m \frac{1}{-i\omega_n+\xi_{\mathbf{k+q}}-\xi_{\mathbf{k}}}\Big(\frac{1}{-i\omega_m+\xi_{\mathbf{k}}}-\frac{1}{-i\omega_{m+n}+\xi_{\mathbf{k+q}}}\Big) \\ &= \frac{2}{L^3}\sum_{\mathbf{k}}\frac{n_f(\epsilon_{\mathbf{k+q}})-n_f(\epsilon_{\mathbf{k}})}{-i\omega_n+\xi_{\mathbf{k+q}}-\xi_{\mathbf{k}}}, \end{aligned} \tag{2.5}$$

where I used that summing over Matsubara frequencies $T\sum_m \frac{1}{i\omega_m-\xi_a} = n_f(\epsilon_a)$. Here $\xi_k = \frac{k^2-k_f^2}{2m}$ measures the energy relative to the Fermi energy.

The sum 2.5 can be transformed into an integral. If the system is isotropic and at zero temperature this integral is better known as the *Lindhard function*. In a one dimensional, static ($\omega_m = 0$) case the result is

$$\begin{aligned}\sum_{\mathbf{k}}\frac{n_f(\epsilon_{\mathbf{k+q}})-n_f(\epsilon_{\mathbf{k}})}{-i\omega_n+\xi_{\mathbf{k+q}}-\xi_{\mathbf{k}}} &\overset{\omega=0}{=} \int\frac{dk}{2\pi}\frac{n_f(\epsilon_{\mathbf{k+q}})-n_f(\epsilon_{\mathbf{k}})}{\cancel{k^2}+2kq+q^2-\cancel{k^2}} \\ &\overset{T=0}{=} \int\frac{dk}{2\pi}\frac{(\Theta(k_f-k+q)-\Theta(k_f-k))}{2kq+q^2} \\ &= \int_{k_f-q}^{k_f}\frac{dk}{2\pi}\frac{1}{2kq+q^2} \\ &= \frac{1}{2q}\log\Big|\frac{2k_f+q}{2k_f-q}\Big|. \end{aligned} \tag{2.6}$$

The above analytic result has the special property that it diverges at $q = 2k_f$. If we look back at 2.5 this is due to a diverging contribution at a nesting vector q that connects two points of the Fermi surface. In this case both particle and hole are on the Fermi surface, $\xi_{k+q} = \xi_k = 0$, and the denominator is zero. In 1d the nesting vector connects the *whole* Fermi surface ($k = -k_f$ and $k = k_f$), this leads to a real singularity in $\chi(q, \omega = 0)$.

The nesting vector also occurs in the higher dimensional cases, but there it represents a point in a larger phase space. As a result the integration over k in higher dimensions, where the the Jacobian gives $d\vec{k} = k^{d-1}dk$, smooths out the divergency.[3]

Allowing $\omega \neq 0$ gives a complex result whose real part still diverges, but the peaks get shifted away from

[3]This is also closely related to the fact that in the dispersion relation in $d = 1$, regardless of its precise nature, can be linearized around the Fermi points.

$q = 2k_f$ (see e.g. [17])

$$\mathrm{Re}\chi(q,\omega) = \frac{1}{4q}\left(\log\left|\frac{1+q_-^2/2q}{1-q_-^2/2q}\right| - \log\left|\frac{1+q_+^2/2q}{1-q_+^2/2q}\right|\right) \qquad \text{with} \qquad q_\pm^2 = \frac{\hbar\omega}{\epsilon_f} \pm q^2. \tag{2.7}$$

This dynamical result is plotted in the figure underneath.

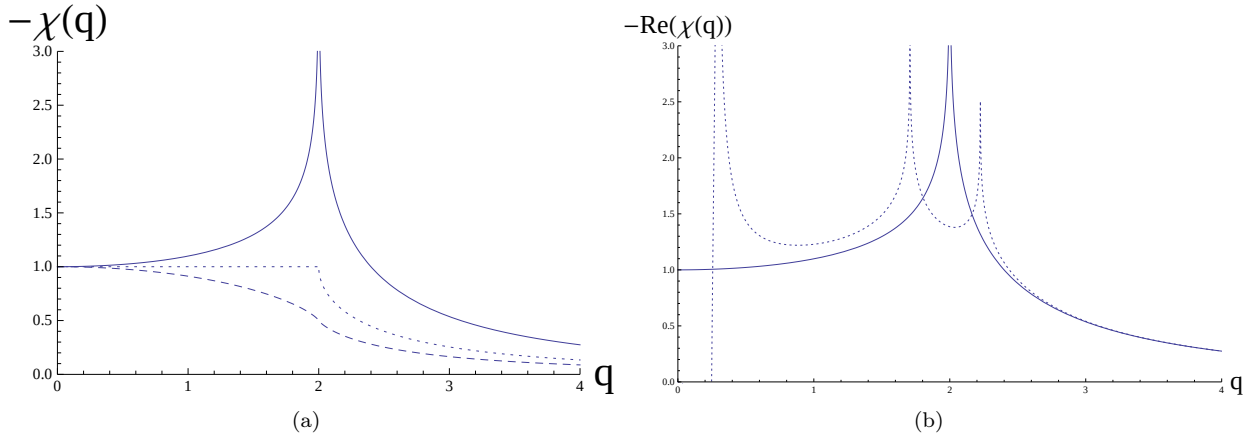

(a) (b)

Figure 2.3: Exact results for the Lindhard function with Fermi momentum put to $k_f = 1$; (a) the static density correlation function $\chi(\vec{q}, \omega = 0)$ for $d = 1$ (solid line) and $d = 3$ (dashed line) as a function of momentum exchange $\vec{q}$. The one dimensional case diverges at $q = 2k_f$. (b) the dynamical density correlation function with $\frac{\hbar\omega}{\epsilon_f} = 0.5$ is depicted by a dotted line. The static result is shown for reference by a solid line.

In 1d a random phase approximation, summing particle-hole bubbles, the total susceptibility takes the form

$$\begin{aligned}\chi &= \chi_0 - \chi_0 V \chi_0 + ... = \sum \chi_0^{n+1}(-V)^n \\ &= \frac{\chi_0}{1+\chi_0 V}.\end{aligned} \tag{2.8}$$

We see that even for an infinitesimal repulsive interaction strength V, the system is on the verge of an instability because at $q = 2k_f$ there is a solution to $\chi_0(\omega = 0, q) = -\frac{1}{V}$.
The divergence of the particle-hole bubbles means that it competes with the superconducting channel (i.e. particle-particle excitations) which is also divergent. Both diagrams try to drive the system into an ordered state (density wave resp. superconducting state), but it is known that such a phase transition does not occur in 1d. To take into account the effect of both types of diagrams one should do a so-called *parquet summation*.

2.3 Luttinger model

Experimental set-ups that realize fermions in one dimension include the quantum Hall liquid edge states [18] and carbon nanotubes [19]. These experimental realization of fermions moving in one dimension ask for a theoretical framework to describe them. As was shown in the previous section, the instability of the Fermi liquid towards any finite interaction makes it an unfavorable starting point to analyze fermions in one dimension. This section introduces the Luttinger model, a model that was specifically designed to describe

the low-energy properties of such systems.
The Tomonaga-Luttinger model assumes a strictly linear dispersion that continues until $E = -\infty$ and all energy levels up to $\pm k_f$ are filled. There are therefore two types particles; there is a branch of left- and a branch of right-movers. The Hamiltonian which realizes this (in the case of interacting spinless fermions) reads

$$H = \sum_{k;r=R,L} v_f(\epsilon_r k - k_f) c^\dagger_{r,k} c_{r,k} + \frac{1}{2\Omega} \sum_{k,k';q} V(q) c^\dagger_{k+q} c^\dagger_{k'-q} c_{k'} c_k, \tag{2.9}$$

where the subscript r specifies left or right moving particles.
Generalization to systems consisting of fermions with spin also exist. In these spinfull models there is a possibility for the spin waves and charge waves to acquire different speeds, a phenomenon called *spin-charge separation*.
In the above Hamiltonian, different scattering processes are denoted by different coupling constants in the Hamiltonian. Forward scattering, a process where two right moving fermions, or two left moving fermions exchange momentum is denoted by g_2 and g_4 (i.e. $(k_f; -k_f) \to (k_f; -k_f)$ and $(k_f; k_f) \to (k_f; k_f)$ processes). Backward scattering involves particles of both left and right moving branches, denoted by g_3.[4]

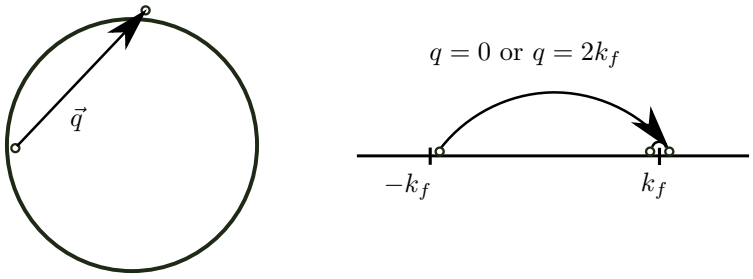

Figure 2.4: Low-lying (near the Fermi surface $E \approx 0$) particle-hole excitations in higher-dimensional set-ups (left), and in the one dimensional case (right). The special Fermi surface topology (two Fermi points), together with the strictly linear dispersion stretching to infinity causes the Tomonaga-Luttinger model to have particle-hole excitations with a well defined energy-momentum relation.

2.3.1 Bosonization

The aforementioned strictly linear dispersion causes any particle-hole excitation to have a well-defined energy-momentum relation. For a right moving particle that is excited from $k \to k + q$ the energy is

$$E(q) = v_f(k + q) - v_f k = v_f q, \tag{2.10}$$

independent of the initial momentum k. Density fluctuations $\rho^\dagger(q) = \sum_k \hat{c}^\dagger_{k+q} \hat{c}_k$, summing over these particle-hole excitations, consist of an even number of fermionic operators and are therefore bosonic in nature. This is the motivation to start seeking for a Hamiltonian reformulated in a bosonic basis. It is easy to see that the interaction term in the Hamiltonian 2.9 written in terms of $\rho(q)$ is quadratic: $H_{int} = \frac{1}{2\Omega} \sum_q V(q)\rho(q)\rho(-q)$.

[4]These are the letters that are usually chosen $\Rightarrow$ *g-ology*.

A formal derivation of the density commutator needs to take into account that a so-called *normal ordering* prescription, $:AB:=AB-\langle 0|AB|0\rangle$. In this way reference to the particle number, an infinite quantity, is avoided. The result is (see e.g. [2])

$$[\rho_r(k),\rho_{r'}(-k')]=-\delta_{k,k'}\delta_{r,r'}\frac{rpL}{2\pi}, \tag{2.11}$$

making the bosonic nature of the density fluctuations manifest. This motivates one to define boson destruction and creation operators as

$$\begin{aligned}\hat{b}_p^\dagger&=\Big(\frac{2\pi}{L|p|}\Big)^{\frac{1}{2}}\big(\Theta(p)\hat{\rho}_R^\dagger(p)+\Theta(-p)\hat{\rho}_L^\dagger(p)\big)\\ b_p&=\Big(\frac{2\pi}{L|p|}\Big)^{\frac{1}{2}}\big(\Theta(p)\hat{\rho}_R^\dagger(-p)+\Theta(-p)\hat{\rho}_L^\dagger(-p)\big).\end{aligned} \tag{2.12}$$

It is even more convenient to express everything in terms of the fields ϕ and θ, which are defined as

$$\begin{aligned}\phi(x)&\equiv-\frac{i\pi}{L}\sum_{p\neq-}\Big(\frac{L|p|}{2\pi}\Big)^{\frac{1}{2}}\frac{1}{p}e^{-\alpha|p|/2-ipx}(\hat{b}_p^\dagger+b_{-p})\\ &=-\frac{i\pi}{L}\sum_{p\neq-}\frac{1}{p}e^{-\alpha|p|/2-ipx}(\hat{\rho}_R^\dagger+\hat{\rho}_L^\dagger)\\ \theta(x)&\equiv\frac{i\pi}{L}\sum_{p\neq-}\frac{1}{p}e^{-\alpha|p|/2-ipx}(\hat{\rho}_R^\dagger-\hat{\rho}_L^\dagger),\end{aligned} \tag{2.13}$$

where in the second line I used 2.12. Also a momentum cutoff α was introduced which should be taken to zero at the end of any calculation.
In terms of these fields the kinetic term of the Hamiltonian reads (once again, see [2] for details)

$$H=\frac{1}{2\pi}\int dx\;\; v_f\Big[\frac{1}{\pi}(\nabla\theta(x))^2+(\nabla\phi(x))^2\Big], \tag{2.14}$$

switching on interactions this becomes

$$H=\frac{1}{2\pi}\int dx\Big[\frac{uK}{\pi}(\nabla\theta(x))^2+\frac{u}{K}(\nabla\phi(x))^2\Big], \tag{2.15}$$

where $u=\frac{1}{2\pi}\sqrt{(2\pi v_f+g_4)^2-g_2^2}$ and $K=\sqrt{\frac{2\pi v_f+g_4-g_2}{2\pi v_f+g_4+g_2}}$ are parameters depending on the different interaction processes.
This is a remarkable result because the kinetic term of this Hamiltonian is quadratic in boson operators ϕ,θ as well. Put differently, through the method of *bosonization* a system of interacting fermions is mapped onto a system of non-interacting bosons. Subsequently all thermodynamic quantities can be computed exactly [20].
This subsection is concluded with two observations that are needed in the following subsection. First of all,

the x derivative of the $\phi(x)$ is the density at $q \sim 0$,

$$\begin{aligned}\nabla\phi(x) &= -\frac{\pi}{L}\sum_{p\neq -} e^{-\alpha|p|/2-ipx}(\hat{\rho}_R^\dagger + \hat{\rho}_L^\dagger) \\ &\overset{\alpha\to 0}{=} -\pi(\rho_R(x)+\rho_L(x)).\end{aligned} \tag{2.16}$$

Secondly, a single particle operator $\psi_r(x) = \sum_k e^{ikx}\hat{c}_k$, destroying a particle at location x, is expressed in terms of the ϕ, θ fields as

$$\psi_r(x) = U_r \lim_{\alpha\to 0} \frac{1}{\sqrt{2\pi\alpha}} e^{irk_f x} e^{-i(r\phi(x)-\theta(x))}. \tag{2.17}$$

Here U_r is a so-called Klein factor to ensure particle conservation. The necessity of this fermionic operator is obvious from the fact that the left-hand side of 2.17 changes the number of fermions by one, whereas the right-hand side, which consists of bosonic operators, conserves the number of fermions. The Klein factors do not have any spacetime dependence and are therefore unimportant when calculating correlation functions [21].

2.3.2 Exact density-density correlation function

The above formalism enables one to give an exact derivation of the scaling of the density-density correlation function at $2k_f$. Consider the density operator,

$$\begin{aligned}\rho(x) &= \psi^\dagger(x)\psi(x) \\ &= \rho_R(x) + \rho_L(x) + \psi_R^\dagger(x)\psi_L(x) + \psi_L^\dagger(x)\psi_R(x) \\ &= -\frac{1}{\pi}\nabla\phi(x) + \frac{1}{2\pi\alpha}\Big(e^{2ik_f x}e^{-2i\phi(x)} + h.c.\Big),\end{aligned} \tag{2.18}$$

where in the last line both 2.16 and 2.17 were used. The equal-time density two-point function reads

$$\langle\rho(x)\rho(0)\rangle = \frac{1}{\pi}\langle\nabla\phi(x)\nabla\phi(0)\rangle + \frac{1}{(2\pi\alpha)^2}\Big(e^{2ik_f x}\langle e^{-2i(\phi(x)-\phi(0))}\rangle + h.c.\Big). \tag{2.19}$$

The first term (q=0) gives $\frac{1}{\pi}\langle\nabla\phi(x)\nabla\phi(0)\rangle = \frac{K}{2\pi^2}\frac{1}{x^2}$, which decays with the same power as the Fermi liquid result, but has a renormalized amplitude depending on the interaction couplings.[5]
To find the $q \sim 2k_f$ behavior, use the identity $\langle e^{i\sum_j A_j\phi(r_j)}\rangle = e^{\frac{1}{2}\langle[\sum_j A_j\phi(r_j)]^2\rangle}$ to rewrite the second term,

$$\langle\rho(x)\rho(0)\rangle = ... + \frac{1}{(2\pi\alpha)^2}\Big(e^{2ik_f x}e^{-2\langle[\phi(x)-\phi(0)]^2\rangle} + h.c.\Big). \tag{2.20}$$

By Fourier decomposing the field $\phi(x)$ the expectation value appearing in the exponential is rewritten as

$$\langle[\phi(x)-\phi(0)]^2\rangle = \frac{1}{\Omega^2}\sum_{q_1,q_2}\langle\phi(q_1)\phi(q_2)\rangle(e^{i(q_1+q_2)x} - e^{iq_1 x} - e^{iq_2 x} + 1). \tag{2.21}$$

[5]The Fourier transform of the first term is the compressibility.

Expressing the expectation values $\langle\phi(q_1)\phi(q_2)\rangle$ as a path integral,

$$\langle\phi(q_1)\phi(q_2)\rangle = \frac{1}{\mathcal{Z}}\int \mathcal{D}\phi(x,\tau)\mathcal{D}\theta(x,\tau)\phi(q_1)\phi(q_2)e^{\frac{1}{\hbar}S}, \tag{2.22}$$

with an action

$$\begin{aligned} S &\overset{2.15}{=} \int_0^\infty d\tau \int dx \frac{i}{\pi}\nabla\theta(x,\tau)\partial_\tau\phi(x,\tau) - \frac{uK}{2\pi}(\nabla\theta(x))^2 + \frac{u}{2\pi K}(\nabla\phi(x))^2 \\ &= \frac{1}{\Omega}\sum_k \frac{-i\mathbf{k}\omega}{\pi}\theta(k)\phi(-k) - \frac{uK\mathbf{k}^2}{2\pi}\theta(k)\theta(-k) + \frac{u\mathbf{k}^2}{2\pi K}\phi(k)\phi(-k), \end{aligned} \tag{2.23}$$

where a Fourier decomposition was done in the the second line. Completing the square,

$$S = \frac{1}{\Omega}\sum_k -\frac{uK\mathbf{k}^2}{2\pi}\left(\theta(k) + \frac{i\omega\phi(k)}{uK\mathbf{k}}\right)\left(\theta(-k) + \frac{i\omega\phi(-k)}{uK\mathbf{k}}\right) - \frac{\omega^2}{2\pi uK}\phi(k)\phi(-k) + \frac{u\mathbf{k}^2}{2\pi K}\phi(k)\phi(-k), \tag{2.24}$$

enables one to integrate out θ. [6] This integration cancels with an equal term originating from the normalization factor $1/\mathcal{Z}$. The resulting expression is a Gaussian integral and can be computed (put $\hbar = 1$),

$$\begin{aligned} \langle\phi(q_1)\phi(q_2)\rangle &= \frac{1}{\mathcal{Z}'}\int \mathcal{D}\phi(x,\tau)\phi(q_1)\phi(q_2)e^{-(2\pi uK\Omega)^{-1}\sum_k \phi(-k)\left(\omega^2+u^2\mathbf{k^2}\right)\phi(k)} \\ &= \frac{\pi uK\Omega\delta_{q_1,-q_2}}{\omega^2 + u^2\mathbf{q_1}^2}. \end{aligned} \tag{2.25}$$

Plugging this result back into 2.21 and transforming sums into integrals,

$$\begin{aligned} \langle[\phi(x)-\phi(0)]^2\rangle &= uK\int d\mathbf{q_1}\int_0^\infty \frac{d\omega}{2\pi}\frac{1}{\omega^2+u^2\mathbf{q_1}^2}(1-\cos\mathbf{q_1}x) \\ &= K\int\frac{d\mathbf{q_1}}{\mathbf{q_1}}(1-\cos\mathbf{q_1}x). \end{aligned} \tag{2.26}$$

To this expression a factor $e^{-\alpha\mathbf{q_1}}$ is added in order to ensure convergence,[7]

$$\begin{aligned} \langle[\phi(x)-\phi(0)]^2\rangle &= K\int\frac{d\mathbf{q_1}}{\mathbf{q_1}}e^{-\alpha\mathbf{q_1}}(1-\cos\mathbf{q_1}x) \\ &= \frac{K}{2}\log\left(1+\frac{x^2}{\alpha^2}\right). \end{aligned} \tag{2.27}$$

Plugging this back into 2.20,

$$\begin{aligned} \langle\rho(x)\rho(0)\rangle &= ... + \frac{1}{(2\pi\alpha)^2}\left(e^{2ik_fx}e^{-K\log\left(1+\frac{x^2}{\alpha^2}\right)} + e^{-2ik_fx}e^{-K\log\left(1+\frac{x^2}{\alpha^2}\right)}\right) \\ &= \frac{K}{2\pi^2}\frac{1}{x^2} + \frac{2}{(2\pi\alpha)^2}\cos(2k_fx)\left(\frac{\alpha}{x}\right)^{2K}, \end{aligned} \tag{2.28}$$

[6] One needs to shift $\theta(k) \to \theta'(k) = \theta(k) - \frac{i\omega\phi(k)}{uK\mathbf{k}}$. Also make the observation that the object $\phi(q_1)\phi(q_2)$, of which we wish to obtain the expectation value, does not depend on θ.

[7] The physical meaning of this cutoff is that it gives a finite bandwidth.

where the last line follows if the momentum cutoff α is taken to zero in the end. The $2k_f$ part is special in the sense that it decays with a non-universal power law depending on the interactions. This is to be compared with the Fermi liquid which would fall of again with $1/x^2$. The special scaling can be seen as the result of a resummation of all the logarithmically divergent diagrams which where discussed in the previous section.

Chapter 3

AdS/CFT and its application to condensed matter

3.1 Indications towards AdS/CFT

The AdS/CFT correspondence tells us that certain field theories can under certain conditions also be described dually by theories on a curved spacetime. What can be said about their relative dimensionality? The observation that the entropy of a black hole is proportional to the area of its horizon (in Planck units) shows that gravitational theories have a number of degrees of freedom which is sub-extensive. The gravitational theory therefore has to be at least one dimension higher, in order to match the degrees of freedom of both theories.[1] The AdS/CFT correspondence is therefore a *holographic correspondence*. It relates a d+1 dimensional anti de Sitter space to a conformal field theory in one dimension less. Both have precisely the same isometries; the conformal group in d dimensions. Via the Gubser-Klebanov-Polyakov-Witten (GPKW) formula

$$\boxed{\langle e^{-\int \phi_0 \mathcal{O}} \rangle_{CFT} = Z_{\text{strings in AdS}}[\phi_0]}, \tag{3.1}$$

which equates the partition sums of the two theories, observables in both theories are in a one-to-one correspondence. It is the subject of the first half of this chapter to explain this formula and its usefulness.

The extra (radial) coordinate of the gravitational theory is usually interpreted as the energy scale at which processes in the field theory take place. In this view the gravitational theory is sliced up in this extra spatial dimension. At each slice lives a CFT with a particular energy scale. Dimensional analysis then tells us the gravitational theory dual to CFT must be invariant under a rescaling $\{x^\mu, r\} \to \{\lambda x^\mu, \frac{r}{\lambda}\}$. It is easy to see that anti de Sitter spacetime, with curvature radius L,

$$ds^2 = -\frac{r^2}{L^2}dt^2 + L^2\frac{dr^2}{r^2} + \frac{r^2}{L^2}dx_i dx^i \tag{3.2}$$

[1] In a QFT one expects: number of states $N \sim e^V \Rightarrow S \sim V$.

is invariant under this scaling. AdS can be seen as a stack of flat spaces (Poincaré symmetry) of increasing size (with r). From the temporal component of the metric $g_{tt} \sim \frac{r^2}{L^2}$ (proper time $d\tau = \sqrt{g_{tt}}dt$) it is clear that the redshift decreases if one moves towards the AdS boundary. This relates the deep interior of AdS to the IR of the CFT and the boundary of AdS to the UV of the CFT.
Anti de Sitter space is the maximally symmetric solution to Einstein's equations resulting from variation of Einstein-Hilbert action,

$$S_{EH} = \frac{1}{2\kappa^2}\int d^{d+1}x\sqrt{-g}\Big(R - 2\Lambda\Big), \tag{3.3}$$

with constant negative curvature Λ. In the case of AdS this cosmological constant is easily shown to take the value $-2\Lambda = \frac{d(d-1)}{L^2}$.

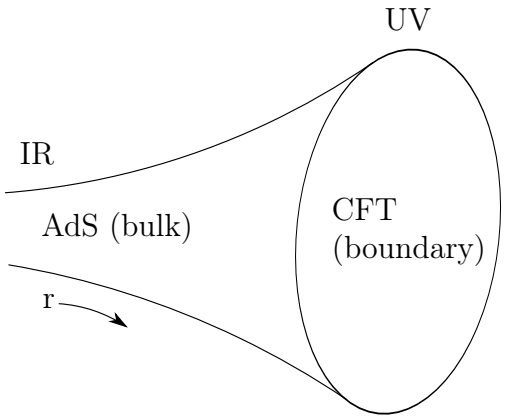

Figure 3.1: Cartoon picture of AdS/CFT. The radial coordinate is interpreted as energy scale.

3.2 The formulation

In the original formulation [22] it was shown that $\mathcal{N} = 4$ supersymmetric $SU(N)$ Yang-Mills theory at large N and strong 't Hooft coupling in 4d is dual to classical type IIB supergravity in 10d on $\mathrm{AdS}_5 \times S^5 + 5$ form flux background. Both have $SO(2,4) \times SO(6)$ as isometry group.
In the year after there followed two articles [23][24] which made the correspondence more precise by relating the correlation functions of gauge invariant operators in the CFT to fluctuating fields in AdS. On the boundary of AdS the bosonic (fermionic) field $\phi(r)$, for example, couples to a bosonic (fermionic) operator $\mathcal{O}$. A change in the field theory is achieved by changing the boundary conditions on the field in the bulk. Changing the mass of the field in the bulk affects the scaling dimension of the operator (see equation 3.7)
Besides scalar and spinor fields, also a graviton field in the bulk couples to an operator on the boundary: the stress-energy tensor $T^{\mu\nu}$. This provides yet another indication that the bulk geometry must have one dimension more. The Weinberg-Witten namely theorem states that a QFT with a conserved stress-energy tensor cannot have massless particles with spin $j > 1$ which carry momentum. The graviton can avoid this by living in a theory defined on a higher-dimensional spacetime.
Say we are interested in the boundary field theory correlation function $\langle \mathcal{O}(x)\mathcal{O}(0)\rangle$ because it represents

an observable of the field theory. The GPKW equation 3.1 enables one to calculate any n-point correlation function by taking functional derivates to the fields ϕ_0 on both sides. The quantity appearing on the right-hand side however is something which can only be approximated. In the context of AdS/CFT this is done by taking a large N limit, where N is the rank of the gauge group on the field theory side, and thereby a measure for the number of degrees of freedom per point. The AdS/CFT correspondence relates this parameter on the bulk side to the inverse Newton constant. In the large N limit quantum corrections are now suppressed with a factor $\frac{L^{d-1}}{G_N} \sim N \gg 1$, and the supergravity partition function is approximated semi-classically by the largest Euclidean saddle,

$$\langle e^{-\int \phi_0 \mathcal{O}} \rangle_{CFT} = \mathcal{Z}_{QG}(\phi_0) \approx e^{-S_{on-shell}[\phi_0]} + \mathcal{O}(1/N). \tag{3.4}$$

In the case of small curvature (that is, the AdS curvature radius L bigger than the energy scale set by the string tension), this on-shell action is given by the Einstein-Hilbert action. Corrections containing higher derivates of the metric than appearing in the Ricci scalar are suppressed in this case.

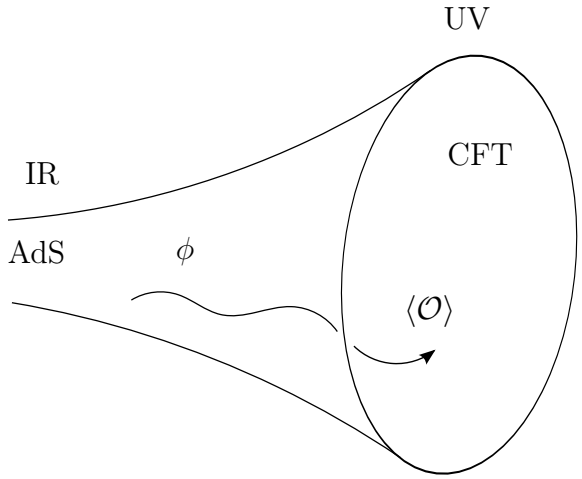

Figure 3.2: Fields in AdS source vev's in the boundary CFT.

The AdS/CFT correspondence is a weak-strong duality. It puts us in a position where processes in the CFT which, due to strong coupling, are hard to solve, can be analyzed in a higher-dimensional space by performing classical gravity calculations. Consider for instance adding a scalar field ϕ to the bulk action. This field is governed by a Klein-Gordon type equation,

$$\Big(\frac{1}{\sqrt{-g}} \partial_r \sqrt{-g} g^{rr} \partial_r + \frac{1}{\sqrt{-g}} \partial_{\tilde{\mu}} \sqrt{-g} g^{\tilde{\mu}\tilde{\nu}} \partial_{\tilde{\nu}} + m^2 \Big) \phi(r, x) = 0, \tag{3.5}$$

where the difference to the usual Klein-Gordon equation lies in the fact that the scalar field now moves on a curved (AdS) background.
The solutions of this equation behave near the boundary as

$$\phi(r, k_\mu) \overset{r \to \infty}{\approx} A(k_\mu) r^{\Delta - d} + B(k_\mu) r^{-\Delta}, \tag{3.6}$$

where the conformal dimension Δ of an operator $\mathcal{O}$ to which ϕ couples on the AdS boundary is the solution to $\Delta(\Delta - d) = m^2L^2$;

$$\Delta_\pm = \frac{d}{2} \pm \sqrt{\left(\frac{d}{2}\right)^2 + (mL)^2}, \tag{3.7}$$

and $\Delta \equiv \Delta_+$.[2] In the case of a vector field the conformal dimensions are determined by $\Delta(\Delta - d + 2) = m^2L^2$. Equation 3.6 shows that near the boundary, the equation of motion has two solutions, a normalizable one (denoted by ϕ_n), which can be excited with finite energy, and a non-normalizable solution (denoted by $\phi_{n.n.}$), which vanishes on the boundary. [3] The normalizable solution ($B(k_\mu)$) corresponds to the expectation value of an operator to which it is dual, while the non-normalizable solution $A(k_\mu)$ indicates that a source for this operator is included in the boundary field theory action. The retarded Green's function describes the reaction of a physical system to a source and is therefore given by the quotient of the subleading to leading term [25],

$$G_R(k_\mu) \sim \frac{B(k_\mu)}{A(k_\mu)}. \tag{3.8}$$

3.3 Connection to condensed matter physics

The AdS/CFT correspondence is only a small part of what can be called gauge/gravity correspondence.[4] One can break the conformal invariance of AdS by introducing additional energy scales. This may lead to a holographic description of strongly coupled systems which are more likely to occur in nature (for a review see [27]). This section contains two such options: temperature and chemical potential. AdS/CMT (CM stands for condensed matter) is especially useful for fermions because strongly coupled fermions are hard to describe analytically and numerical simulations at finite density are not possible because of the "sign problem".

A convenient way to put the boundary field theory at finite temperature is to use an asymptotically AdS black hole geometry. This makes use of the observation of Bekenstein and Hawking [28] that black holes are thermodynamical objects. I will discuss this option in 3.3.1. Another way to include temperature is by introducing a thermal gas of particles. Above a certain temperature the black hole solution is preferred [29]. The second option for introducing an additional energy scale is to consider a nonzero chemical potential for a charge density on the boundary. This procedure, the subject of 3.3.2, leads to a charged black hole in the bulk. Another way to describe the boundary field theory at finite charge density, is to let a fluid of electrons, instead of the black hole, carry a macroscopic amount of charge outside the horizon, see e.g. [30]

[2] Negative masses are allowed as long as they do not violate the *Breitenlohner-Freedman bound* $m_{BF} = -\left(\frac{d}{2}\right)^2$ [31]. Below this bound the conformal dimensions become imaginary in which case there a no normalizable solutions.

[3] Also there exist a mass range between BF and unitarity bound where there are two normalizable solutions. This allows for an *alternative quantization* switching the role of expectation value and source.

[4] A nice example is described in [26] where it was proven that the quasi-normal modes of certain black holes, the eigenfrequencies of a "ringing" black hole subject to a perturbation, coincide with the poles of the retarded Green's function of the CFT. These are two independent, analytic calculations which give the same result.

3.3.1 Temperature

Reconsider the Einstein-Hilbert action with a negative cosmological constant,

$$S_{EH} = \frac{1}{2\kappa^2}\int d^{d+1}x\sqrt{-g}\Big(R - 2\Lambda\Big) \qquad -2\Lambda = \frac{d(d-1)}{L^2}. \tag{3.9}$$

If one drops the demand of scale invariance and looks for solutions to the Einstein equations (which follow from variation of the action) which are spherically symmetric and invariant under spacetime translations, there exist also black hole solutions of the form [5]

$$ds^2 = -r^2 f(r)dt^2 + \frac{dr^2}{r^2 f(r)} + r^2 dx_i^2 \qquad f(r) = 1 - \Big(\frac{r_h}{r}\Big)^d. \tag{3.10}$$

There is a black hole horizon at r_h, $f(r_h) = 0$, in whose vicinity light becomes infinitely redshifted.[6] The black hole is asymptotically AdS $\Big(g_{tt} \overset{r\to\infty}{=} \frac{r^2}{L^2}\Big)$ which was demanded by the negative cosmological.[7]

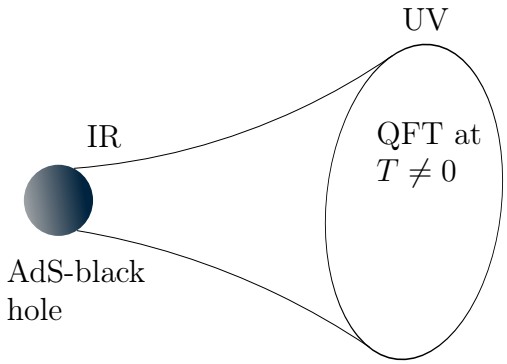

Figure 3.3: An asymptotically AdS-black hole geometry describes a field theory at finite temperature.

The so-called *warpfunction* has a near horizon expansion

$$\begin{aligned} f(r) &\overset{r\to r_h}{=} \cancel{f(r_h)} + |f'(r_h)|(r - r_h) + \mathcal{O}\big((r-r_h)^2\big) \\ &= \frac{dr_h^d}{r_h^{d+1}}(r - r_h) = \frac{d}{r_h}(r - r_h), \end{aligned} \tag{3.11}$$

so the near horizon metric becomes

$$ds^2 \overset{r\to r_h}{\approx} -r_h d(r - r_h)dt^2 + \frac{dr^2}{r_h d(r - r_h)} + r_h^2 d\vec{x}^2. \tag{3.12}$$

Consider a variable change $\varkappa = \frac{dr_h}{2}$ and $\rho = \frac{2}{\sqrt{r_h d}}\sqrt{r - r_h}$. This gives

$$\varkappa^2\rho^2 = r_h d(r - r_h), \tag{3.13}$$

[5] Via the AdS/CFT correspondence, static black holes correspond to ensembles with strongly interaction constituent particles, *in equilibrium*.

[6] Interpreting the radial coordinate as the RG scale, the black hole horizon functions as an IR cutoff. This is a geometric realization of a energy gap in dual the field theory.

[7] This is to be compared to the fact that the Schwarzschild black hole is asymptotically flat.

and also

$$d\rho = \frac{1}{\sqrt{r_h d}} \frac{1}{\sqrt{r - r_h}} dr \qquad \Rightarrow \qquad d\rho^2 = \frac{1}{r_h d(r - r_h)} dr^2. \tag{3.14}$$

Putting the parts together leads to the metric

$$ds^2 \approx -\varkappa^2 \rho^2 dt^2 + d\rho^2 + \frac{L^2}{z_h^2} d\vec{x}^2. \tag{3.15}$$

Doing a Wick rotation to Euclidean space we note that 3.15 looks just like flat space in polar coordinates. In fact the metric is singular at $\rho = 0$ but the geometry is regular provided that the polar angle has period 2π. Demanding the absence of a conical singularity at $r = r_h$, we therefore have to identify the polar angle with $\varkappa\tau \simeq \varkappa\tau + 2\pi$ where $\tau = \frac{1}{T}$. A periodicity in the time component in Euclidean signature is interpreted as temperature ($e^{-iHt} \to e^{-H\beta}$)

Conclusion: the black hole has a temperature

$$\boxed{T = \frac{\varkappa}{2\pi} = \frac{1}{4\pi} \frac{|\partial f(r)|}{\partial r}\bigg|_{r=r_h}}. \tag{3.16}$$

3.3.2 Finite density

Consider a field theory at finite density, i.e. with a nonzero chemical potential μ. In order to describe this system holographically, a gauge field $A_\mu(r \to \infty, x, t)$ is introduced in the AdS bulk. The AdS/CFT dictionary namely tells us that the asymptotic value of this gauge field $A_\mu(r \to \infty, x, t) = \mathcal{A}_\mu(x, t)$ couples to a conserved four-current J^μ on the boundary, and thereby sets a nonzero chemical potential μ for a net charge in the boundary field theory. This entry of the dictionary shows that gauged symmetries in the bulk appear as global symmetries on the boundary.

The gauge field in the bulk is introduced by adding to the Einstein Hilbert action a Maxwell term (see equation 4.1). The Einstein equations then obtain a nonzero stress-energy term depending on the gauge fields, and thereby become coupled Einstein-Maxwell equations. As a result of the introduction of a gauge field the black hole solutions carry a charge.[8] The conclusion is that the boundary field theory can obtain a finite charge density if a charged black hole is used on the bulk side. Another way to view this is that a charge density on the boundary induces a flux in the bulk. This flux disappears behind the horizon which leads to the conclusion that the black hole must carry a charge.

3.4 Renormalization and double trace deformations

Via the AdS/CFT correspondence we hope to gain insight in the dynamics of a strongly coupled many-body systems. While the microscopic behavior of all constituent particles is extremely complicated, observables in condensed matter are measured at macroscopic length and time scales. It turns out that often the macroscopic behavior is largely insensitive to the dynamics of the individual particles. The microscopic degrees of freedom can then be integrated out in the sense of the Wilsonian approach to renormalization

[8] The identification of charge is made by an ADM calculation.

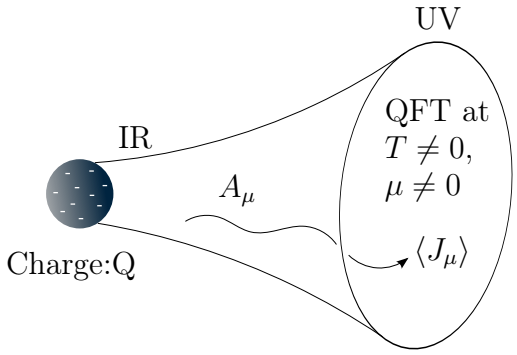

Figure 3.4: An asymptotically AdS charged black hole geometry describes a field theory at finite temperature and finite charge density.

and these affect the IR only via a finite amount of relevant and marginal couplings.
Recently this was given an interpretation on the gravity side [32] [33]. This interpretation relies on the observation that in AdS/CFT the radial direction of the bulk is related to the energy scale of the CFT. The aforementioned increasing redshift in the deep interior of AdS leads to the conclusion that low-energy processes are captured by the region near the black hole horizon $r \approx r_h$, with the black hole functioning as a cutoff. In analogy to the Wilsonian approach of the renormalization of field theory, where the high energies are integrated out, in the bulk AdS space the bulk action would be integrated out over the radial direction. This integration will end at some IR scale which in our zero temperature BTZ case is set by the boundary of the near horizon $AdS_2 \times \mathbb{R}$ geometry (to be discussed in the next chapter). In this way all the UV information is captured in a boundary term that appears in the action.[9]

3.5 Historical overview of AdS/CMT

The AdS/CFT duality provides a convenient framework to describe strongly coupled condensed matter problems. This approach was initiated by [35], who used holography to describe the transport properties of hydrodynamics (momentum transport), culminating in a viscosity to entropy density ratio of $\frac{\eta}{s} = \frac{1}{4\pi}$.
The year after, in 2008, Hartnoll, Herzog and Horowitz introduced the concept of the Holographic superconductor [36] [37]. They observed the 'condensation' of a scalar field in a Reisner-Nordström black hole geometry if the Breitenlohner-Freedman bound is violated. This happens when the conformal dimension of the scalar field becomes imaginary. This condensation, the occurrence of a nonzero expectation value for the scalar field, is interpreted in the boundary field theory as the onset of superconductivity, precisely as in the Landau formalism of superconductivity where the breaking of a symmetry is associated with a phase transition. The black hole is now said to be 'dressed by scalar hair'.
One year later, in 2009, a MIT group [5][38] and the group in Leiden [39] independently found signatures of Fermi surfaces on the gravity side of the duality. These Fermi surfaces where signaled by peaks in the boundary spectral function. The dual field theories where named 'non-Fermi liquids from holography'. These publications led to a search for new quantum states of matter. The question arises whether there are

[9] We have assumed that the CFT was not deformed by double trace deformations, even though they can represent relevant operators which therefore should not be ignored [34]. In [32] it was observed that even if one starts with a zero double trace coupling κ under the renormalization flow this coupling obtains a non-zero value.

other phases, besides the ones which are already known, which have not been discovered yet. AdS/CFT provides one with a plethora of different quantum states of matter, most of which probably do not have anything to do with the real world. The challenge now is to classify the relevant ones.

Chapter 4

The Charged BTZ black hole

The BTZ black hole was first developed by Bañados, Teitelboim and Zanelli in [4]. With the holographic description of low-dimensional spinless fermion systems as our goal, the focus is on the black hole solution without angular momentum but with charge. A charged black hole is required to describe the boundary field theory at finite density (see subsection 3.3.2). A rotating (Kerr-AdS) black hole could be used whenever one wishes to describe a boundary field theory with a nonzero chemical potential for particles with spin or magnetic moment.

Classical AdS_3 gravity combined with electro-magnetism is described by the Einstein-Hilbert action with a Maxwell term and a negative cosmological constant,

$$S_{EH}[A,g] = \frac{1}{2\kappa^2}\int d^{2+1}x\sqrt{-g}\Big(R + \frac{2}{L^2} - \frac{L^2}{g_f^2}F^2\Big). \tag{4.1}$$

Varying this action gives the coupled Einstein-Maxwell equations

$$\begin{aligned} &R_{\mu\nu} - \frac{R}{2}g_{\mu\nu} - \frac{1}{L^2}g_{\mu\nu} = \frac{\kappa^2}{2g_f^2}\Big(2F_{\mu\sigma}F^{\sigma}_{\nu} - \frac{1}{2}F_{\sigma\rho}F^{\sigma\rho}\Big), \\ &D_\mu F^{\mu\nu} = 0. \end{aligned} \tag{4.2}$$

The aim of this chapter is to find a solution to these equations which is spherically symmetric, static and which has a non-vanishing electrical field on the boundary, where the metric should asymptote to AdS_3. We first turn our attention to the gauge field in the bulk which sources the right-hand side of the above equation.

4.1 Gauge field

Because we are interested only in electronic properties we put the magnetic part of the electromagnetic tensor to zero: $F_{r\phi} = 0$. Also due to spherical symmetry we take $F_{t\phi} = 0$. We restrict to a gauge $A_r = A_x = 0$. The solution for A_t is found by solving the Maxwell equation. In the region near the boundary $r \to \infty$ we know that the metric is asymptotically AdS $-g_{tt}(r) = g^{rr}(r) = \frac{r^2}{L^2}$. We will see (in the next subsection)

that we can find a consistent solution be taking $-g_{tt}(r) = g^{rr}(r)$ for all r,

$$\begin{aligned} D^\mu F_{\mu\nu} &= \frac{1}{\sqrt{-g}}\partial_M(\sqrt{-g}g^{MA}g^{ZB}F_{AB}) \\ &= \frac{1}{r}\partial_r r g^{rr} g^{tt} F_{rt} = 0 \\ &= \partial_r^2 A_t(r) + \frac{1}{r}\partial_r A_t(r) = 0 \qquad \rightarrow A_t = A_t^{(1)}\log r + A_t^{(0)}. \end{aligned} \tag{4.3}$$

The above derivation is equivalent to the statement that the Poisson equation ($\nabla \cdot E = \frac{\rho}{\epsilon}$) in 2 dimensions has the solution $A_t(r) = Q \ln \frac{r}{l}$, where Q is the total charge of the black hole and also a length scale l was introduced on dimensional grounds.

Among the other ways to find this log-behavior is a $d = 2 + \epsilon \rightarrow 2$ limit of the Reisner-Nordström gauge field $A_t(r) = \mu\left(1 - \left(\frac{r_h}{r}\right)^{d-2}\right)$ [40].[1]

Also note that the naive application of the aforementioned $\Delta(\Delta - d + 2) = m^2L^2$ equation (see section 3.2) in order to find the conformal dimension of an operator coupling to a massless vector field, in the case of AdS_3, leads to a near boundary field expansion

$$A_t(r \rightarrow \infty) \sim A_t^{(1)} r^{\Delta_-} + A_t^{(0)} r^{\Delta_+}, \tag{4.4}$$

with $\Delta_- = \Delta_+ = 0$, i.e. two constants. The fact however that A_μ is the solution to a second order differential equation demands two independent solutions. This problem can only be fixed by the appearance of a log-term.

In this last argument the log behavior appears only in the asymptotic expansion of the gauge field whereas the first two arguments given are true for all r. In general the leading terms of the gauge field near the AdS boundary ($r \rightarrow \infty$) are

$$A_t(r) = A_t^{(1)}\log r + A_t^{(0)} + ... \tag{4.5}$$

As shown in equation 4.3, this expression is exact (no dots) in the case of pure gravity. In the case of additional matter content in the form of e.g. scalar or Dirac hair, the right-hand side of that equation obtains additional terms such that the gauge field expansion is true only near the boundary.

The integration constants in the above solution can be completely fixed by imposing boundary conditions. First of all, the no-hair theorem states that the black hole should be fully specified by its mass, charge and angular momentum. This means that gauge field vanishes on the black hole horizon, setting the relation between the constants $A_i^{(0)} = -A_i^{(1)}\log r_h$. The second boundary condition makes use of the leading/subleading analysis discussed in the previous chapter. Naive application indicates that $A_t^{(1)} = \mu$ and $A_t^{(0)} = \rho$. [2] The correct analysis however switches these two quantities [41].[3]

The above choices fix the gauge and consequently the non-vanishing gauge field on the boundary has physical relevance for it is associated to a global symmetry in the field theory.

---

[1] Do a rescaling $\mu \rightarrow \mu' = \frac{\mu}{d-2}$ and take $\epsilon \rightarrow 0$ to see that $A_t(r) = \mu'\left(1 - e^{\epsilon \log \frac{r_h}{r}}\right) = \mu \ln \frac{r}{r_h}$.

[2] Via an ADM calculation one could also express everything in terms of the charge Q of the black hole (bulk quantity) instead of the boundary quantities ρ and μ which were chosen here.

[3] Thanks to Juan Jottar for pointing this out. An indication that this is correct is the fact that in the $d \rightarrow 2$ limit the logarithmic term arose from the subleading term.

4.2 Solving Einstein's equations

Now that we have obtained the gauge field, the stress-energy tensor $T_{\mu\nu} = -\left(F_\mu{}^\psi F_{\psi\nu} + \frac{1}{4} g_{\mu\nu} F_{\psi\tau} F^{\psi\tau}\right)$ has non-vanishing components $T_{tt} = \frac{1}{2} g(r) \frac{Q^2}{r^2}$ and $T_{rr} = -\frac{1}{2f(r)} \frac{Q^2}{r^2}$. We will calculate various components of the Einstein equation for a general space time which will lead us to the conclusion that in three space time dimensions the charged BTZ is the unique solution. Start with the most general static (time independent), spherically symmetric metric,

$$ds^2 = -f(r)dt^2 + \frac{dr^2}{g(r)} + r^2 d\phi^2, \tag{4.6}$$

Our aim is to determine the functions $f(r)$ and $g(r)$. Using Mathematica (see appendix B) we calculate the components of the Einstein tensor $G_{\mu\nu} = R_{\mu\nu} - \frac{1}{2} g_{\mu\nu} R$,

$$G_{tt} = -\frac{f(r)\partial_r g(r)}{2r} \tag{4.7}$$

$$G_{rr} = \frac{\partial_r f(r)}{2r f(r)}. \tag{4.8}$$

$G_{\phi\phi}$ is also non-vanishing but I don't need that component for my arguments. Einstein's equation for these components reads

$$-\frac{1}{l^2} f(r) + \frac{1}{2} g(r) \frac{Q^2}{r^2} + \frac{f(r)\partial_r g(r)}{2r} = 0 \qquad (tt) - \text{component} \tag{4.9}$$

$$-\frac{1}{g(r) l^2} + \frac{1}{2} \frac{Q^2}{f(r) r^2} + \frac{\partial_r f(r)}{2r f(r)} = 0 \qquad (rr) - \text{component}. \tag{4.10}$$

Comparing the (tt) and (rr) components we see that $f(r)\partial_r g(r) = g(r)\partial_r f(r)$ so that $\partial_r \ln f(r) = \partial_r \ln g(r)$.[4] Up to a multiplicative factor which can be absorbed by a redefinition of the time coordinate we see that $f(r) = g(r)$. This function is found subsequently by inspection of the Einstein equation,

$$-\frac{1}{l^2} + \frac{1}{2} \frac{Q^2}{r^2} + \frac{\partial_r f(r)}{2r} = 0$$

$$\partial_r f(r) = \frac{2r}{l^2} - \frac{1}{2} \frac{2Q^2}{r}. \tag{4.11}$$

The integration constant is interpreted via the ADM formalism as the mass M [42],

$$\boxed{f(r) = \frac{r^2}{l^2} - M - \frac{1}{2} Q^2 \ln\left(\frac{r}{l}\right)}. \tag{4.12}$$

This correctly retrieves the asymptotic ($r \to \infty$) AdS_3 boundary, where the metric has 1+1 dimensional conformal symmetry. At large frequencies $\omega \gg \mu$ (in the UV) the effects of finite density are therefore washed out and one recovers the conformal invariance of a zero density system (a vacuum).

[4] To see this, multiply the rr-component with $f(r)g(r)$.

4.3 Near horizon analysis of extremal BTZ

The charged BTZ metric, in units where the AdS radius is put to $L = 1$ and where the mass is scaled out, reads

$$\boxed{ds^2 = -f(r)dt^2 + \frac{dr^2}{f(r)} + r^2 dx^2 \qquad f(r) = r^2 - 1 - \frac{Q^2}{2}\log r \qquad A_t(r) = \rho \log r}. \quad (4.13)$$

The black hole has an outer horizon at $r = r_h = 1$ ($f(1) = 0$), independent of the black hole charge Q. The temperature (see: section 3.3.1) of the black hole $4\pi T = \frac{\partial f(r)}{\partial r}\big|_{r=r_h} = 2r - \frac{Q^2}{2r}\big|_{r=1}$ vanishes if the black hole is extremely charged (Q=2). In this case the inner and outer horizon merge, and the warpfunction of an extremely charged black hole has a double zero at the horizon, [5]

$$\begin{aligned} f(r) &\overset{r\to r_h}{\approx} f(r_h) + (r - r_h)\frac{\partial f(r)}{\partial r}\bigg|_{r=r_h} + \frac{1}{2}(r - r_h)^2 \frac{\partial^2 f(r)}{\partial r^2}\bigg|_{r=r_h} \\ &= 2(r - r_h)^2. \end{aligned} \quad (4.14)$$

This double zero turns out to be the reason for an interesting near horizon geometry. Putting back the

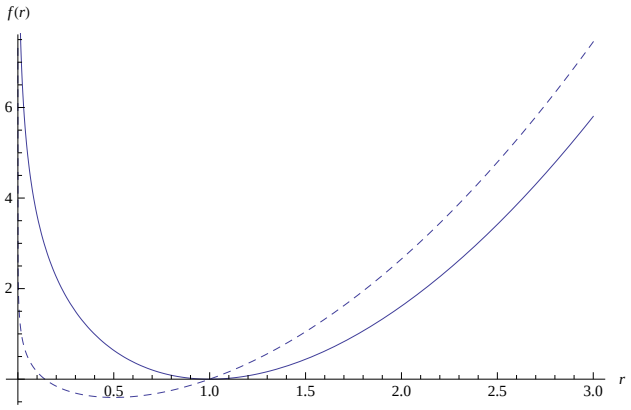

Figure 4.1: The warpfactor $f(r)$ is depicted for Q=1 (dashed), Q=2 (solid).

expansion of the warpfunction into the metric 4.13 gives

$$ds^2 = -2(r-1)^2 dt^2 + \frac{dr^2}{2(r-1)^2} + dx^2. \quad (4.15)$$

Define a near horizon radial coordinate $\zeta = \frac{\lambda L_2^2}{r-1}$, $t = \lambda^{-1}\tau$ and take the limits $\lambda \to 0$ and ζ, τ finite. Notice that finite τ corresponds to a long time limit. This means that ω which is the variable conjugate to t goes to zero. This is equivalent to the statement that the near horizon geometry is associated with the IR physics. The variable change gives

$$d\zeta = d\left(\frac{\lambda L_2^2}{r-1}\right) = -\frac{\lambda L_2^2}{(r-1)^2} dr, \quad (4.16)$$

[5] Further increase of Q will lead a black hole horizon at $r_h > 1$ but this charge regime is non physical.

leading to

$$\frac{L_2^2}{\zeta^2}d\zeta^2 = \frac{L_2^2(r-1)^2}{\lambda^2 L_2^4}\frac{\lambda^2 L_2^4}{(r-1)^4}dr^2 = \frac{L_2^2}{(r-1)^2}dr^2 = \frac{1}{2(r-1)^2}dr^2. \tag{4.17}$$

We also see that

$$-\frac{L_2^2}{\zeta^2}d\tau^2 = -\frac{L_2^2(r-1)^2}{L_2^2\lambda^2}\lambda^2 dt^2 = -2(r-1)^2 dt^2. \tag{4.18}$$

Collecting these terms and comparing with 4.15 we see that the near horizon geometry of the BTZ black hole is given by

$$ds^2 = \frac{L_2^2}{\zeta^2}(-d\tau^2 + d\zeta^2) + \frac{dx^2}{L_2^2}, \tag{4.19}$$

which is $\mathrm{AdS}_2 \times \mathbb{R}$ with an AdS_2 radius $L_2 = \frac{1}{\sqrt{2}}L = \frac{1}{\sqrt{2}}$.

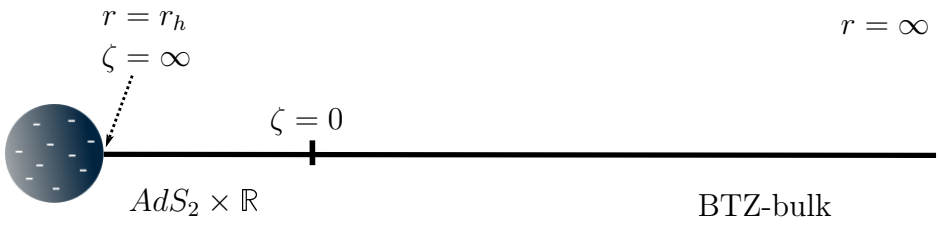

Figure 4.2: Various regions of BTZ spacetime.

The form $\mathrm{AdS}_2 \times \mathbb{R}^{n-1}$ also occurs in higher-dimensional AdS black holes (see e.g. [5]). This subsection thereby shows the analogy between the BTZ black hole and higher-dimensional extremely charged AdS black holes. The Reisner-Nordström black hole for example has a near horizon $AdS_2 \times \mathbb{R}^2$ geometry.
The occurance of the AdS factor hints at an emergent conformal symmetry. Put differently, it may be the case that this region is dual to some $0+1$d CFT. The implications of this near horizon have been the study of some recent papers, most notably [43] and let to the introduction of the so-called *semi-local quantum liquid*.
The extremal BTZ black hole with the $\mathrm{AdS}_2 \times \mathbb{R}$ near horizon geometry has a finite horizon area and thereby a non-zero Bekenstein-Hawking entropy density $S = \frac{A}{4G}$. To my knowledge, there is no conclusive resolution found for the violation of the third law of thermodynamics caused by this large ground state degeneracy. A possible way out of this problem is that this near horizon geometry corresponds to an intermediate quantum state and that for smaller values of r we have a (Lifschitz) AdS_4 geometry; the black hole has disappeared and in the absence of a horizon there is zero entropy density. Another possible answer is that it is a large N artifact: tunneling interactions, lifting degeneracy, are suppressed at large N.

Chapter 5

Fermions in a BTZ background

The BTZ black hole, which was discussed extensively in the previous chapter, is a solution to the equations of motions which follow from varying the Einstein-Hilbert-Maxwell action with negative cosmological constant,

$$S_{EH}[A,g] = \frac{1}{2\kappa^2}\int d^{2+1}x\sqrt{-g}\Big(R + \frac{2}{L^2} - \frac{L^2}{g_f^2}F^2\Big). \tag{5.1}$$

We introduce fermionic matter fields in the bulk of this geometry by adding to the action a term

$$S_{fermion} = \int d^3x\sqrt{-g}i(\bar{\Psi}\Gamma^\mu D_\mu\Psi - m\bar{\Psi}\Psi), \tag{5.2}$$

with $D_\mu = \partial_\mu + \frac{1}{4}\omega_{ab\mu}\Gamma^{ab} - iqA_\mu$, where $\Gamma^{ab} = \frac{1}{2}[\Gamma^a, \Gamma^b]$. We work in the probe limit which means that the fermionic fields do not back-react on the metric. Varying the above action leads to a Dirac equation in a BTZ background (section 5.1), with the necessary spin connection terms due to the non-vanishing curvature. In section 5.2 the near horizon geometry of the BTZ is examined in more detail. It turns out that in that region the Dirac equation can be solved exactly.[1] Section 5.3 discusses the matching procedure for which a numerical study in the full background geometry is required.[2]

5.1 Dirac equation and Spin connection

Decomposing the spinor in Fourier modes $\Psi = \Psi(r)e^{-i\omega t+ikx}$, the Dirac equation reads

$$\Big(\Gamma^t(-i\omega + \frac{1}{4}\omega_{abt}\Gamma^{ab} - iqA_t) + \Gamma^r\partial_r + \Gamma^x(ik + \frac{1}{4}\omega_{abx}\Gamma^{ab}) - m\Big)\Psi(r) = 0. \tag{5.3}$$

Bulk indices are denoted by Greek letters $\mu = (r, \hat{\mu})$, where hatted Greek letters indicate directions along the boundary $\hat{\mu} = (t, x)$. Because the gamma matrices in $\Gamma^\mu\partial_\mu = e_a^\mu\Gamma^a\partial_\mu$ can only be defined in flat space, tangent spacetime indices $(a, b, ..)$ are used. Also the underlined indices $(\underline{t}, \underline{r}, \underline{x})$ refer to this tangent space.

[1] I give an explicit analytic derivation of the low dimensional generalization of a formula which appears in the literature but of which I have not found any derivations[5].

[2] This method was introduced by the MIT group in [5].

The vielbeins, defined through $g_{\mu\nu} = \eta_{ab} e^a_\mu e^b_\nu$, in the case of the BTZ metric are

$$e^{\underline{t}}_{\ t} = \sqrt{-g_{tt}} = \sqrt{f} \qquad e^{\underline{r}}_{\ r} = \sqrt{g_{xx}} = \frac{1}{\sqrt{f}} \qquad e^{\underline{x}}_{\ x} = \sqrt{g_{rr}} = r. \tag{5.4}$$

We will now show that the the spin connection, given by

$$\omega^{ab}_\mu = e^a_\nu \partial_\mu e^b_\sigma g^{\sigma\nu} + e^a_\nu e^b_\tau g^{\tau\sigma} \Gamma^\nu_{\sigma\mu}, \tag{5.5}$$

can be removed by a rescaling of the spinor fields. *The derivation we present only requires that (i) the metric components are related via $g_{tt} = -g_{rr}^{-1}$, and that (ii) the metric components only depend on the radial coordinate r.*
The Christoffel symbols $\Gamma^\sigma_{\mu\nu} = \frac{1}{2} g^{\sigma\rho}(\partial_\mu g_{\rho\nu} + \partial_\nu g_{\mu\rho} - \partial_\rho g_{\mu\nu})$ in that case are

$$\begin{aligned} \Gamma^r_{rr} &= \frac{1}{2} g^{rr} \partial_r g_{rr} \qquad \Gamma^r_{tt} = -\frac{1}{2} g^{rr} \partial_r g_{tt} \qquad \Gamma^r_{xx} = -\frac{1}{2} g^{rr} \partial_r g_{xx} \\ \Gamma^t_{tr} = \Gamma^t_{rt} &= \frac{1}{2} g^{tt} \partial_r g_{tt} \qquad \Gamma^x_{xr} = \Gamma^x_{rx} = \frac{1}{2} g^{xx} \partial_r g_{xx}. \end{aligned} \tag{5.6}$$

Because the metric is diagonal the first term in 5.5 is only non-vanishing when $\sigma = \nu \Rightarrow a = b$: This gives

$$\begin{aligned} \omega^{\underline{tt}}_{\underline{r}} &= e^{\underline{t}}_{\ t} \partial_r e^{\underline{t}}_{\ t} g^{tt} + e^{\underline{t}}_{\ t} e^{\underline{t}}_{\ t} g^{tt} \Gamma^t_{tr} \\ &= \sqrt{-g_{tt}} \partial_r \sqrt{-g_{tt}} g^{tt} + \sqrt{-g_{tt}} \sqrt{-g_{tt}} g^{tt} \Gamma^t_{tr} \\ &= \frac{1}{2} \frac{\sqrt{-g_{tt}}}{(-g_{tt})^{\frac{3}{2}}} \partial_r(-g_{tt}) - \frac{1}{2} g^{tt} \partial_r g_{tt} = 0, \end{aligned} \tag{5.7}$$

and analogously $\omega^{\underline{rr}}_{\underline{r}} = \omega^{\underline{xx}}_{\underline{r}} = 0$.
There are however four Christoffel connections left with which the non-vanishing components of the spin connection can be constructed,

$$\begin{aligned} \omega^{\underline{rt}}_{\underline{t}} &= e^{\underline{r}}_{\ r} e^{\underline{t}}_{\ t} g^{tt} \Gamma^r_{tt} = \cancel{\sqrt{g_{rr}} \sqrt{-g_{tt}}} g^{tt} (-\frac{1}{2} g^{rr} \partial_r g_{tt}) = -\frac{1}{2} \partial_r (\sqrt{-g_{tt}})^2 = -\frac{\partial_r \sqrt{-g_{tt}}}{\sqrt{g_{rr}}} \\ \omega^{\underline{tr}}_{\underline{t}} &= e^{\underline{t}}_{\ t} e^{\underline{r}}_{\ r} g^{rr} \Gamma^t_{rt} = \cancel{\sqrt{-g_{tt}} \sqrt{g_{rr}}} g^{rr} (\frac{1}{2} g^{tt} \partial_r g_{tt}) = -\frac{1}{2} \partial_r g_{tt} = \frac{\partial_r \sqrt{-g_{tt}}}{\sqrt{g_{rr}}} \\ \omega^{\underline{rx}}_{\underline{i}} &= e^{\underline{r}}_{\ r} e^{\underline{x}}_{\ x} g^{ii} \Gamma^r_{xx} = \sqrt{g_{rr}} \sqrt{g_{xx}} g^{xx} (-\frac{1}{2} g^{rr} \partial_r g_{xx}) = -\frac{1}{2} \sqrt{g^{rr}} \sqrt{g^{xx}} \partial_r g_{xx} = -\frac{\partial_r \sqrt{g_{xx}}}{\sqrt{g_{rr}}} \\ \omega^{\underline{xr}}_{\underline{i}} &= e^{\underline{x}}_{\ x} e^{\underline{r}}_{\ r} g^{rr} \Gamma^x_{rx} = \sqrt{g_{xx}} \sqrt{g_{rr}} g^{rr} (\frac{1}{2} g^{xx} \partial_r g_{xx}) = \frac{\partial_r \sqrt{g_{xx}}}{\sqrt{g_{rr}}}. \end{aligned} \tag{5.8}$$

Lower indices with $\omega_{ab\mu} = \eta_{ac} \eta_{bd} \omega^{cd}_{\ \ \mu}$,

$$\omega_{\underline{rtt}} = -\omega_{\underline{trt}} = \frac{\partial_r \sqrt{-g_{tt}}}{\sqrt{g_{rr}}} \qquad \omega_{\underline{rxx}} = -\omega_{\underline{xrx}} = -\frac{\partial_r \sqrt{g_{ii}}}{\sqrt{g_{rr}}}. \tag{5.9}$$

In this BTZ case (D=2+1) the gamma matrices are 2×2 and can conveniently be chosen to coincide with the Pauli matrices, where an additional factor i in $\Gamma^{\underline{t}}$ has to be taken into account in order to satisfy the

Clifford algebra.[3] With the choice $\Gamma^{\underline{t}} = i\sigma^1$, $\Gamma^{\underline{r}} = \sigma^3$ and $\Gamma^{\underline{x}} = \sigma^2$, the Dirac equation 5.3 is purely real and therefore the spinor solutions are purely real. Now using the commutation relation for Pauli matrices $[\sigma_a, \sigma_b] = 2i\epsilon_{abc}\sigma_c$, with our choice of gamma matrices we have $-\Gamma^{\underline{t}}\Gamma^{\underline{tr}} = \Gamma^{\underline{r}}\Gamma^{\underline{rr}} = \Gamma^{\underline{x}}\Gamma^{\underline{xr}} = \Gamma^{\underline{r}}$. This allows us to write the spin connection term in the action as

$$\begin{aligned}\frac{1}{4}\omega_{ab\mu}\Gamma^{\mu}\Gamma^{ab} &= \frac{1}{4}\sqrt{-g^{tt}}\Gamma^{\underline{t}}\omega_{\underline{r}\underline{t}\underline{t}}\Gamma^{\underline{r}\underline{t}} + \frac{1}{4}\sqrt{-g^{tt}}\Gamma^{\underline{t}}\omega_{\underline{t}\underline{r}\underline{t}}\Gamma^{\underline{t}\underline{r}} + \frac{1}{4}\sqrt{g^{xx}}\Gamma^{\underline{x}}\omega_{\underline{r}\underline{x}\underline{x}}\Gamma^{\underline{r}\underline{x}} + \frac{1}{4}\sqrt{g^{xx}}\Gamma^{\underline{x}}\omega_{\underline{x}\underline{r}\underline{x}}\Gamma^{\underline{x}\underline{r}} \\ &= \frac{1}{2}\Gamma^{\underline{t}}\sqrt{-g^{tt}}\frac{\partial_r\sqrt{-g_{tt}}}{\sqrt{g_{rr}}}\Gamma^{\underline{r}\underline{t}} - \frac{1}{2}\Gamma^{\underline{x}}\sqrt{g^{xx}}\frac{\partial_r\sqrt{g_{xx}}}{\sqrt{g_{rr}}}\Gamma^{\underline{r}\underline{x}} \\ &= \frac{1}{2}\sqrt{-g^{tt}}\frac{\partial_r\sqrt{-g_{tt}}}{\sqrt{g_{rr}}}\Gamma^{\underline{r}} + \frac{1}{2}\sqrt{g^{xx}}\frac{\partial_r\sqrt{g_{xx}}}{\sqrt{g_{rr}}}\Gamma^{\underline{r}}, \end{aligned} \tag{5.10}$$

which can subsequently be written as

$$\begin{aligned}\frac{1}{4}\omega_{ab\mu}\Gamma^{\mu}\Gamma^{ab} &= \frac{1}{2}\frac{1}{\sqrt{g_{rr}}}\Gamma^{\underline{r}}\frac{1}{\sqrt{-g_{tt}g_{ii}}}\partial_r\sqrt{-g_{tt}g_{xx}} \\ &= \frac{1}{\sqrt{g_{rr}}}\Gamma^{\underline{r}}\partial_r \ln\left(\frac{-g}{g_{rr}}\right)^{1/4}. \end{aligned} \tag{5.11}$$

Taking into account the above considerations on the spin connection, the Dirac equation 5.3 now turns into

$$\Big(\sqrt{-g^{tt}}\Gamma^{\underline{t}}(-i\omega - iqA_t) + \sqrt{g^{rr}}\Gamma^{\underline{r}}\partial_r + \sqrt{g^{xx}}\Gamma^{\underline{x}}ik - m + \frac{1}{\sqrt{g_{rr}}}\Gamma^{\underline{r}}\partial_r \ln\Big(\frac{-g}{g_{rr}}\Big)^{1/4}\Big)\Psi = 0. \tag{5.12}$$

A rescaling of the spinors $\Psi = \left(\frac{-g}{g_{rr}}\right)^{-1/4}\psi$ transforms the spin connection into

$$\frac{1}{\sqrt{g_{rr}}}\Gamma^{\underline{r}}\partial_r \ln\Big(\frac{-g}{g_{rr}}\Big)^{1/4}\Psi = \frac{1}{4}\frac{1}{\sqrt{g_{rr}}}\Gamma^{\underline{r}}\Big(\frac{-g}{g_{rr}}\Big)^{-5/4}\Big(\partial_r\frac{-g}{g_{rr}}\Big)\psi. \tag{5.13}$$

The result of this rescaling is a complete cancellation of the spin connection by a term that originates from the r-derivative term in the Dirac equation,

$$\sqrt{g^{rr}}\Gamma^{\underline{r}}\partial_r\Psi = \underbrace{\sqrt{g^{rr}}\Big(\frac{-g}{g_{rr}}\Big)^{-1/4}\Gamma^{\underline{r}}\partial_r\psi}_{\text{stays in Dirac equation}} \underbrace{- \frac{1}{4}\sqrt{g^{rr}}\Gamma^{\underline{r}}\Big(\frac{-g}{g_{rr}}\Big)^{-5/4}\partial_r\Big(\frac{-g}{g_{rr}}\Big)\psi}_{\text{gives cancellation}}. \tag{5.14}$$

The result is a Dirac equation

$$\Big(\sqrt{-g^{tt}}\Gamma^{\underline{t}}(-i\omega - iqA_t) + \sqrt{g^{rr}}\Gamma^{\underline{r}}\partial_r + \sqrt{g^{xx}}\Gamma^{\underline{x}}ik - m\Big)\psi = 0, \tag{5.15}$$

which for large r asymptotes to [4]

$$\Big(r\sigma_3\partial_r - m\Big)\psi = 0. \tag{5.16}$$

[3] In general the Dirac equation equation in D dimensional space time has $2^{D/2} \times 2^{D/2}$ dimensional gamma matrices when D is even and $2^{(D-1)/2} \times 2^{(D-1)/2}$ dimensional gamma matrices when D is odd.

[4] Use here that $\sqrt{-g^{tt}}, \sqrt{g^{xx}} \sim \frac{1}{r} \to 0$.

We find a asymptotic solution of the form $\psi(r) \overset{r\to\infty}{\longrightarrow} \psi^- r^{-m} \begin{pmatrix} 0 \\ 1 \end{pmatrix} + \psi^+ r^m \begin{pmatrix} 1 \\ 0 \end{pmatrix}$.

After scaling back with $\Psi = \left(\frac{-g}{g_{rr}}\right)^{-1/4} \psi \overset{r\to\infty}{=} r^{-\frac{d}{2}} \psi$ this solution reads

$$\Psi(r) \overset{r\to\infty}{\longrightarrow} \Psi^- r^{-1-m} \begin{pmatrix} 0 \\ 1 \end{pmatrix} + \Psi^+ r^{-1+m} \begin{pmatrix} 1 \\ 0 \end{pmatrix}. \tag{5.17}$$

This shows that the general large r solution for a fermion in the background of a higher-dimensional AdS black hole, $\Psi(r) \overset{r\to\infty}{\longrightarrow} \Psi^- r^{-\frac{d}{2}-m} + \Psi^+ r^{-\frac{d}{2}+m}$, also applies in the case of the BTZ black hole.

5.2 Boundary Green's function of $\mathrm{AdS}_2 \times \mathbb{R}$

In 4.3 it was found that the extremal BTZ black hole has an $\mathrm{AdS}_2 \times \mathbb{R}$ near horizon geometry,

$$ds^2 = \frac{l_2^2}{\zeta^2}(-d\tau^2 + d\zeta^2) + \frac{dx^2}{l_2^2}, \tag{5.18}$$

which is parametrized by the radial coordinate $\zeta = \frac{L_2^2}{r-1}$. The gauge field $A_t(r) = \rho \ln r$ has a near horizon expansion $A_t(r \to 1) = \rho(\cancel{\ln 1} + (r-1)) = \frac{\rho}{\zeta}$.[5] This section covers the Dirac equation for fermions in this specific region of the BTZ geometry.

The spin connection is removed by the same rescaling $\Psi = \left(\frac{-g}{g_{rr}}\right)^{-1/4} \psi$. This is because the metric written in the usual radial coordinate 4.15 clearly satisfies the two demands posed in the previous section. Decomposing the field $\Psi = \left(\frac{-g}{g_{rr}}\right)^{-1/4} e^{-i\omega\tau + ikx}\psi(\zeta)$, the Dirac equation takes the form

$$\begin{aligned} &\Big(e^t_{\ \underline{t}}\Gamma^{\underline{t}}(\partial_t - iqA_t) + e^{\zeta}_{\ \underline{\zeta}}\Gamma^{\underline{\zeta}}\partial_\zeta + e^x_{\ \underline{x}}\Gamma^{\underline{x}}\partial_x - m\Big)\psi = 0 \\ &\quad \Big(\sigma_1(\omega + qA_t) + \sigma_3\partial_\zeta + \frac{R_2}{\zeta}(\sigma_2 ik - m)\Big)\psi = 0. \end{aligned} \tag{5.19}$$

Multiplying from the right with σ_3 and using $\sigma_3\sigma_3 = \mathbb{1}$, $\sigma_3\sigma_1 = -i\sigma_2$, $\sigma_3\sigma_2 = -i\sigma_1$ gives

$$\partial_\zeta\psi = i\sigma_2\Big(\omega + \frac{q\rho}{\zeta}\Big)\psi + \frac{R_2}{\zeta}(-\sigma_1 k + \sigma_3 m)\psi. \tag{5.20}$$

Near the $\mathrm{AdS}_2 \times \mathbb{R}$ boundary when $\zeta \to 0$ the equation takes the form

$$\zeta\partial_\zeta\psi = \begin{pmatrix} m & q\rho - k \\ -q\rho - k & -m \end{pmatrix}\psi, \tag{5.21}$$

which is solved by

$$\begin{aligned} &\psi(\zeta) = A_+\psi_+\zeta^{\nu_k} + A_-\psi_-\zeta^{-\nu_k} \\ &\Rightarrow \Psi(\zeta) = A_+\psi_+\zeta^{\frac{1}{2}+\nu_k} + A_-\psi_-\zeta^{\frac{1}{2}-\nu_k}, \end{aligned} \tag{5.22}$$

[5] In units where the black hole horizon is scaled to $r_h = 1$, the gauge field vanishes on the horizon if $\mu = 0$.

where $\nu_\pm = \pm\sqrt{m^2+k^2-(q\rho)^2}$ (and $\nu_+ \equiv \nu_k$) are the eigenvalues and $\psi_\pm = \begin{pmatrix} \nu_\pm + m \\ q\rho + k \end{pmatrix}$ are the eigenvectors of the above matrix. In the second line there was a scaling back $\Psi = \left(\frac{-g}{g_{rr}}\right)^{-1/4}\psi = \zeta^{\frac{1}{2}}\psi$.
The quotient of the constants $A_\pm$ is the retarded Green's function, with the additional demand that the solution should be infalling near the horizon. We find this quotient by solving the Dirac equation 5.20 in the whole $\mathrm{AdS}_2 \times \mathbb{R}$ geometry. After setting $R_2 = 1$ and rescaling the spinors $\psi \to \frac{1}{\sqrt{2}}(1-i\sigma_1)\psi$ this Dirac equation reads

$$\begin{aligned}(1-i\sigma_1)\zeta\partial_\zeta\psi &= (i\sigma_2+\sigma_2\sigma_1)(\omega\zeta+q\rho)\psi + (\sigma_3 - i\sigma_3\sigma_1)m\psi + i(1+i\sigma_1)k\psi \\ (1-i\sigma_1)\zeta\partial_\zeta\psi - (1+i\sigma_1)ik\psi &= (\sigma_2-\sigma_3)i(\omega\zeta+q\rho)\psi + (\sigma_3+\sigma_2)m\psi, \end{aligned} \tag{5.23}$$

where in the second line I used $\sigma_a\sigma_b = \delta_{ab} + i\epsilon_{abc}\sigma_c$. Writing this as a matrix equation

$$\begin{pmatrix} 1 & -i \\ -i & 1 \end{pmatrix}\zeta\partial_\zeta\psi - \begin{pmatrix} 1 & i \\ i & 1 \end{pmatrix} ik\psi = \begin{pmatrix} -1 & -i \\ i & 1 \end{pmatrix} i(\omega\zeta+q\rho)\psi + \begin{pmatrix} 1 & -i \\ i & -1 \end{pmatrix} m\psi, \tag{5.24}$$

makes it easier to read of the components,

$$\begin{aligned} &(A) \qquad \zeta\partial_\zeta\psi_1 - i\zeta\partial_\zeta\psi_2 - ik\psi_1 + k\psi_2 = -i(\omega\zeta+q\rho)\psi_1 + (\omega\zeta+q\rho)\psi_2 + m\psi_1 - im\psi_2 \\ &(B) \qquad \zeta\partial_\zeta\psi_1 + i\zeta\partial_\zeta\psi_2 + ik\psi_1 + k\psi_2 = -i(\omega\zeta+q\rho)\psi_1 - (\omega\zeta+q\rho)\psi_2 - m\psi_1 - im\psi_2, \end{aligned} \tag{5.25}$$

where the component (B) was multiplied with i. Adding these two (and dividing by 2) gives

$$(C) \qquad \Big[\zeta\partial_\zeta + i(\omega\zeta+q\rho)\Big]\psi_1 = -(k+im)\psi_2 \qquad \Rightarrow \qquad \psi_2 = \frac{\Big[\zeta\partial_\zeta + i(\omega\zeta+q\rho)\Big]\psi_1}{-(k+im)}, \tag{5.26}$$

while subtracting (B) of (A) (and dividing by $-2i$) gives

$$(D) \qquad \Big[\zeta\partial_\zeta - i(\omega\zeta+q\rho)\Big]\psi_2 = -(k-im)\psi_1 \qquad \Rightarrow \qquad \psi_1 = \frac{\Big[\zeta\partial_\zeta - i(\omega\zeta+q\rho)\Big]\psi_2}{-(k-im)}. \tag{5.27}$$

Plugging ψ_2 in (D) gives

$$\begin{aligned} \Big[\zeta\partial_\zeta - i(\omega\zeta+q\rho)\Big]\Big[\zeta\partial_\zeta + i(\omega\zeta+q\rho)\Big]\psi_1 &= (k+im)(k-im)\psi_1 \\ \zeta\partial_\zeta\Big(\zeta\partial_\zeta\psi_1\Big) + \cancel{i(\omega\zeta+q\rho)\zeta\partial_\zeta\psi_1} + i\omega\zeta\psi_1 - \cancel{i(\omega\zeta+q\rho)\zeta\partial_\zeta\psi_1} &= \Big(m^2+k^2-(\omega\zeta+q\rho)^2\Big)\psi_1 \\ \zeta^2\partial_\zeta^2\psi_1 + \zeta\partial_\zeta\psi_1 &= \Big(\nu^2 - \omega\zeta(2q\rho+i) - (\omega\zeta)^2\Big)\psi_1, \end{aligned} \tag{5.28}$$

whereas plugging ψ_1 into (C) gives the same expression for ψ_2 except for one minus sign,

$$\zeta^2\partial_\zeta^2\psi_2 + \zeta\partial_\zeta\psi_2 = \Big(\nu^2 - \omega\zeta(2q\rho - i) - (\omega\zeta)^2\Big)\psi_2. \tag{5.29}$$

Note that given a solution for ψ_1, the other spinor component ψ_2 is determined via equation 5.26. We can therefore focus attention on the differential equation 5.28 governing ψ_1.

The term with the first derivative $\partial_\zeta \psi$ can be removed by a redefinition $\psi \to A\psi$,

$$\zeta^2\Big(A\partial_\zeta^2\psi_1 + \cancel{2\partial_\zeta A\partial_\zeta\psi_1} + \psi_1\partial_\zeta^2 A\Big) + \Big(\cancel{\zeta A\partial_\zeta\psi_1} + \zeta\psi_1\partial_\zeta A\Big) = \Big(\nu^2 - \omega\zeta(2q\rho + i) - (\omega\zeta)^2\Big)A\psi_1, \quad (5.30)$$

giving an equation which fixes A,

$$2\zeta^2\partial_\zeta A + \zeta A = 0 \qquad \Rightarrow A = \frac{1}{\sqrt{\zeta}}. \quad (5.31)$$

Dividing the whole equation 5.30 by A gives

$$\zeta^2\Big(\partial_\zeta^2\psi_1 + \psi_1\frac{1}{A}\partial_\zeta^2 A\Big) + \zeta\psi_1\frac{1}{A}\partial_\zeta A = \Big(\nu^2 - \omega\zeta(2q\rho + i) - (\omega\zeta)^2\Big)\psi_1. \quad (5.32)$$

The terms containing A are easily calculated ($\frac{1}{A}\partial_\zeta A = -\frac{1}{2\zeta}$ and $\frac{1}{A}\partial_\zeta^2 A = \frac{3}{4\zeta^2}$) and plugged in, yielding

$$\partial_\zeta^2\psi_1 + \Big(\omega^2 + 2i\omega\frac{(\frac{1}{2} - iq\rho)}{\zeta} + \frac{\frac{1}{4} - \nu^2}{\zeta^2}\Big)\psi_1 = 0, \quad (5.33)$$

which is solved by [6]

$$\psi_1(\zeta) = A_1 W_{\frac{1}{2} - iq\rho,\nu}(2i\omega\zeta) + B_1 W_{-\frac{1}{2} + iq\rho,\nu}(-2i\omega\zeta). \quad (5.34)$$

Expressing Whittaker's function in terms of the Kummer's confluent hypergeometric function

$$W_{k,\mu}(z) = e^{-\frac{z}{2}} z^{\mu + \frac{1}{2}} U(\mu - \kappa + \frac{1}{2}, 1 + 2\mu; z), \quad (5.35)$$

the solution for ψ_1 is written as

$$\psi_1(\zeta) = \quad = A_1 e^{-i\omega\zeta}(2i\omega\zeta)^{\nu + \frac{1}{2}} U(\nu + iq\rho, 1 + 2\nu; 2i\omega\zeta) + B_1 e^{i\omega\zeta}(-2i\omega\zeta)^{\nu + \frac{1}{2}} U(\nu - iq\rho + 1, 1 + 2\nu; -2i\omega\zeta). \quad (5.36)$$

To find the *retarded* Green's function, the solution should be infalling near the horizon. The term scaling like $\phi \sim e^{-i\omega(\tau - \zeta)} \sim e^{i\omega\zeta}$ satisfies this (as τ grows, so must ζ, to keep the phase fixed). Therefore $A_1 = 0$. We could now use a cute trick

$$U(a, b, z) = \frac{\Gamma(1 - b)}{\Gamma(a - b + 1)} M(a, b, z) + \frac{\Gamma(b - 1)}{\Gamma(a)} z^{1 - b} M(a - b + 1, 2 - b, z), \quad (5.37)$$

[6] Recall that the Whittaker function $W_{k,\mu}(z)$ is the solution to

$$\frac{d^2 w}{dz^2} + \big(-\frac{1}{4} + \frac{k}{z} + \frac{\frac{1}{4} - \mu^2}{z^2}\big)w = 0,$$

to rewrite U in terms of M

$$U(\nu - iq\rho + 1, 1 + 2\nu; -2i\omega\zeta) = \frac{\Gamma(-2\nu)}{\Gamma(1 - iq\rho - \nu)} M(\nu - iq\rho + 1, 1 + 2\nu; -2i\omega\zeta) + \frac{\Gamma(2\nu)}{\Gamma(1 - iq\rho + \nu)} (-2i\zeta\omega)^{-2\nu} M(1 - iq\rho - \nu, 1 - 2\nu; -2i\zeta\omega). \quad (5.38)$$

In the asymptotic boundary limit $\zeta \to 0$ the hypergeometric function M goes to 1, so the infalling piece of ψ_1 has a near boundary expansion that reads,[7]

$$\psi_1 \overset{\zeta \to 0}{=} e^{i\omega\zeta}(-2i\omega\zeta)^{\frac{1}{2}+\nu} \frac{\Gamma(-2\nu)}{\Gamma(1 - iq\rho - \nu)} + e^{i\omega\zeta}(-2i\omega\zeta)^{\frac{1}{2}-\nu} \frac{\Gamma(2\nu)}{\Gamma(1 - iq\rho + \nu)}. \quad (5.39)$$

The rescalings $\Psi = \left(\frac{-g}{g_{rr}}\right)^{-1/4} \psi = \zeta^{\frac{1}{2}} \psi$ and $\psi \to A\psi = \frac{\psi}{\sqrt{\zeta}}$ cancel each others effect. Also the transformation $\psi \to \frac{1}{\sqrt{2}}(1 - i\sigma_1)\psi$ must be undone. This is done by observing $\frac{1}{\sqrt{2}}(1 - i\sigma_1)\frac{1}{\sqrt{2}}(1 + i\sigma_1) = 1$. The eigenspinors appearing in equation 5.22 are therefore transformed into

$$(1 + i\sigma_1)\psi_\pm = (1 + i\sigma_1) \begin{pmatrix} \nu_\pm + m \\ q\rho + k \end{pmatrix} = \begin{pmatrix} \nu_\pm + m + iq\rho + ik \\ i\nu_\pm + im + q\rho + k \end{pmatrix}. \quad (5.40)$$

We effectively put unity in equation 5.20. One term $\frac{1}{\sqrt{2}}(1 - i\sigma_1)$ turned the Dirac equation into a hypergeometric equation, the other term transformed the eigenspinor. The solution on the asymptotic boundary reads

$$\Psi_1 \overset{\zeta \to 0}{=} e^{i\omega\zeta}(-2i\omega\zeta)^{\frac{1}{2}+\nu}(\nu + m + iq\rho + ik) \frac{\Gamma(-2\nu)}{\Gamma(1 - iq\rho - \nu)} + e^{i\omega\zeta}(-2i\omega\zeta)^{\frac{1}{2}-\nu}(-\nu + m + iq\rho + ik) \frac{\Gamma(2\nu)}{\Gamma(1 - iq\rho + \nu)}. \quad (5.41)$$

Conclusion: The exact boundary retarded Green's function for a fermion of mass m and charge q in $AdS_2 \times \mathbb{R}$ is[8]

$$\boxed{\mathcal{G}(\omega, k) = \frac{\Gamma(-2\nu)\Gamma(1 - iq\rho + \nu)}{\Gamma(2\nu)\Gamma(1 - iq\rho - \nu)} \frac{m + ik + iq\rho + \nu}{m + ik + iq\rho - \nu} (2\omega)^{2\nu} e^{-i\pi\nu}} \quad (5.42)$$

This result is to be compared with [5]. The reason for the similarity in the expressions found traces back to the fact that BTZ and Reisner-Nordström black holes have the same near horizon gauge field expansion. Notation $\mathcal{G}_k(\omega) = c(k)\omega^{2\nu_k} = |c(k)|e^{i\gamma_k}\omega^{2\nu_k}$ is introduced, to single out the interesting scaling in ω. Also the subscript k in ν_k is restored.

5.3 Boundary Green's function of full background

To find the retarded Green's function of the full BTZ geometry, the solution found in the region near the black hole horizon (henceforth denoted by $\Psi_I(r)$) needs to be matched to solutions that live in the rest of the geometry (denoted by $\Psi_O(r)$). Recall that at $\omega = 0$, a solution to the Dirac equation was found in the

[7] $M(a, b, \zeta \to 0) = \frac{\Gamma(b)}{\Gamma(a)\Gamma(a-b)} \int_0^1 e^{\zeta u} u^{a-1}(1 - u)^{b-a-1} du = \frac{\Gamma(b)}{\Gamma(a)\Gamma(a-b)} B(a, b) = 1.$

[8] This is found by taking the quotient of subleading to subleading term of 5.41. Also $(-i)^{2\nu} = (-1)^\nu = e^{-i\pi\nu}$ was used.

near horizon region which scales as [9]

$$\Psi_I(\zeta) = \psi_+ \zeta^{\frac{1}{2}+\nu_k} + \psi_- \zeta^{\frac{1}{2}-\nu_k}. \tag{5.43}$$

Matching this to the outer region solution means that

$$\Psi_O(r) \overset{r\to r_h}{\sim} (r-1)^{-\frac{1}{2}+\nu_k} + \mathcal{G}_k (r-1)^{-\frac{1}{2}-\nu_k}. \tag{5.44}$$

is demanded, where $\mathcal{G}_k(\omega)$ is the Green's function of the IR $AdS_2 \times \mathbb{R}$ derived in the previous subsection. On the other hand, the retarded Green's function of the full geometry is given by the ratio of leading to sub-leading terms near the AdS-boundary. This is the motivation to expand the near horizon solution in terms of near boundary solutions (found in equation 5.17).

$$\begin{aligned} \Psi_O(r) \quad &\overset{r\to\infty}{=} \quad \underbrace{(r-1)^{-\frac{1}{2}+\nu_k}}_{a_+ r^{-1-m} + b_+ r^{-1+m}} + \mathcal{G}_k \quad \underbrace{(r-1)^{-\frac{1}{2}-\nu_k}}_{a_- r^{-1-m} + b_- r^{-1+m}} \\ &= \quad \big(a_+ + a_- \mathcal{G}_k\big) r^{-1-m} + \big(b_+ + b_- \mathcal{G}_k\big) r^{-1+m} \end{aligned} \tag{5.45}$$

In this expansion appear coefficients a and b (depending on k) which are found by solving the full outer region equations of motion numerically. The result is an expression for the retarded Green's function,

$$G_R(k) \sim \frac{b_+ + b_- \mathcal{G}_k}{a_+ + a_- \mathcal{G}_k}. \tag{5.46}$$

This strict $\omega = 0$ result is generalized in [5] to include small nonzero ω, [10]

$$G_R(\omega, k) = K \frac{b_+^{(0)} + \omega b_+^{(1)} + O(\omega^2) + \mathcal{G}_k(\omega)\big(b_-^{(0)} + \omega b_-^{(1)} + O(\omega^2)\big)}{a_+^{(0)} + \omega a_+^{(1)} + O(\omega^2) + \mathcal{G}_k(\omega)\big(a_-^{(0)} + \omega a_-^{(1)} + O(\omega^2)\big)}. \tag{5.47}$$

Once again, the a's and b's are coefficients that are found by solving the full outer region equations of motion numerically. Numerical studies (see e.g. [43]) have shown that there are certian momentum values k_f such that $a_+^{(0)}(k_f) = 0$. This motivates us to make an $\omega \approx 0, k \approx k_f$ expansion. The latter means that $a_+^{(0)}(k) \approx \cancel{a_+^{(0)}(k_f)} + (k - k_f)\frac{\partial a_+^{(0)}(k)}{\partial k}$, leading to

$$G_R(\omega, k \approx k_f) \approx \frac{h_2}{k_\perp - \frac{1}{v_f}\omega - h_2 e^{i\gamma_{k_f}} \omega^{2\nu_{k_f}}}, \tag{5.48}$$

where $v_f \equiv -\frac{\partial_k a_+^{(0)}(k_f)}{a_+^1(k_f)}$, $h_1 \equiv \frac{b_+^1(k_f)}{\partial_k a_+^{(0)}(k_f)}$ and $h_2 \equiv -|c(k_f)| \frac{a_-^0(k_f)}{\partial_k a_+^{(0)}(k_f)}$. The term that scales nontrivially in ω is the IR $AdS_2 \times \mathbb{R}$ Green's function $\mathcal{G}_k(\omega)$ which appears as the self-energy.

[9] Equation 5.35 shows that ω always comes in pairs with ζ, therefore $\zeta \to 0$ and $\omega \to 0$ are equivalent.

[10] The factor K is a term not depending on k and scaling as $K \sim \mu^{2\nu_U}$ where ν_U is the conformal dimension of the boundary operators $\nu_U = \sqrt{m^2 R^2 + \frac{d^2}{4}} = \sqrt{m^2 R^2 + 1}$.

Chapter 6

Quantum Corrections

The fermionic action introduced in the previous chapter

$$S_{fermion} = \int d^3x\sqrt{-g}i(\bar{\Psi}\Gamma^{\mu}\Big(\partial_{\mu} + \frac{1}{4}\omega_{ab\mu}\Gamma^{ab} - iqA_{\mu}\Big)\Psi - m\bar{\Psi}\Psi), \tag{6.1}$$

contains a gauge field-fermion-fermion interaction term which is 1/N suppressed. Moving away from large N allows fermion/anti-fermion bubbles (depicted in figure 6) which contribute to the gauge field two-point function (denoted by $\tilde{\chi}$).

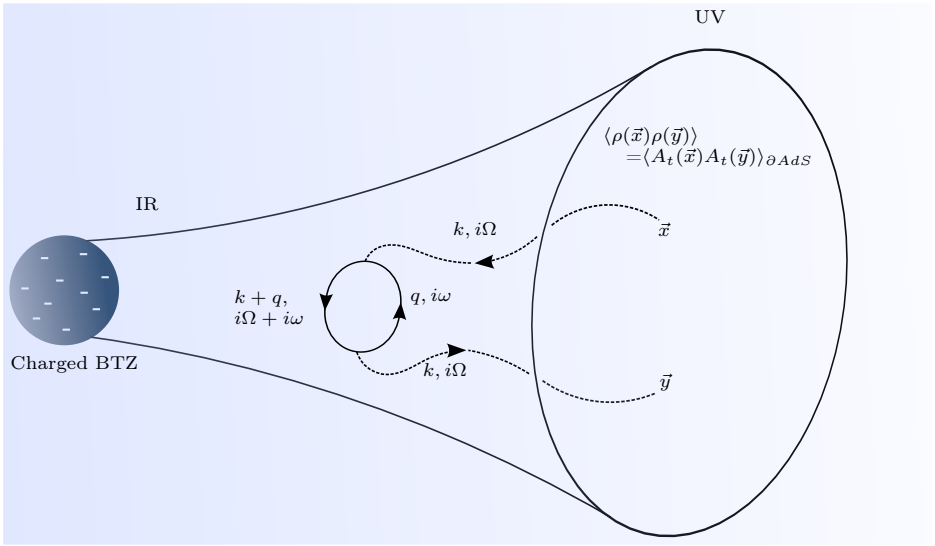

Figure 6.1: Fermionic loop correction to the gauge field two-point function.

The fermions can be formally be integrated out from the action

$$\begin{aligned} S &= \int d^{2+1}x \mathrm{Tr}\ \ln(i\not{D}_0 + m + iq\not{A}) \\ &= \int d^{2+1}x \mathrm{Tr}\ \ln\Big(D_0(r,\vec{x},r',\vec{x}')^{-1} + iq\not{A}\Big) \\ &\sim \int d^{2+1}x \mathrm{Tr}\ \ln\Big(1 + D_0(r,\vec{x},r',\vec{x}')iq\not{A}\Big), \end{aligned} \tag{6.2}$$

where we absorbed the term $\mathrm{Tr}\ \ln\Big(D_0(r,\vec{x},r',\vec{x}')^{-1}\Big)$ into the constant in front of the partition sum. Expanding out for small coupling q,[1]

$$\begin{aligned} S = \int d^{2+1}x \mathrm{Tr}\Big(D_0(r,\vec{x},r',\vec{x}')iq\not{A}\Big) \\ - \frac{1}{2}\int d^{2+1}x \int d^{2+1}x' \mathrm{Tr}\Big(D_0(r,\vec{x},r',\vec{x}')iq\not{A}D_0(r',\vec{x}',r,\vec{x})iq\not{A} + ..\Big). \end{aligned} \tag{6.3}$$

The first order term gives a tadpole diagram which contributes to the background gauge field. The second order term is the diagram we are interested in. We aim at the calculation of quantum corrections to $\langle\rho(r)\rho(0)\rangle = \langle J_0(r)J_0(0)\rangle = \langle A_t(r\to\infty,\vec{x})A_t(r\to\infty,0)\rangle$. Therefore only the $\mu,\nu = t$ components are of interest. Fourier transforming the propagators with

$$D(r,\vec{x},r',\vec{x}') = \int \frac{d\omega}{2\pi}\int \frac{dk}{2\pi} D(r,r',i\omega,k)e^{-i\omega(\tau-\tau')+ik(x-x')}, \tag{6.4}$$

gives the amplitude of the one loop diagram (In Euclidean signature),

$$\tilde{\chi}(i\omega,q) \equiv \frac{(iq)^2}{2}\int dr\sqrt{g}\,dr'\sqrt{g'}\int \frac{d\Omega\,dk}{(2\pi)^2} A_t(r,-q)\mathrm{Tr}\Big[\Gamma^t D(i\Omega,k,r,r')\Gamma^t D(i\Omega+i\omega,k+q,r',r)\Big]A_t(r',q) \tag{6.5}$$

In the above expression appear fermionic bulk to bulk propagators $D(i\Omega,k,r,r')$. The next section discusses their construction. Because the gauge field only depends on the radial coordinate, henceforth the q dependance is omitted.
In section 6.2 the one loop diagram is further manipulated and the radial parts are integrated out. Under some simplifications, an analytic solution to the resulting integral is found in section 6.3.

6.1 Construction of fermionic propagator

Written in position space ($\vec{x} = x,t$) the bulk to bulk propagator $D(r,\vec{x},r',\vec{x}')$ obeys the usual Green's function equation [27],

$$(\not{D} - m)D(r,\vec{x},r',\vec{x}') = \frac{i}{\sqrt{g}}\delta(r-r')\delta(\vec{x}-\vec{x}'). \tag{6.6}$$

[1] Use $\log(1+x) \overset{x\to 0}{=} x - \frac{x^2}{2} + \mathcal{O}(x^3)$.

Fourier transforming the boundary coordinates into momentum space gives

$$(\Gamma^r D_r - m)D(r, r', \Omega, k) = \frac{i}{\sqrt{g}}\delta(r - r'). \tag{6.7}$$

In curved spacetime the non-trivial vielbeins make it very difficult (if possible) to find general expressions for these propagators. One needs expressions for geodesic distances which are not easy to obtain analytically, especially in non-radial cases. Via tedious calculations and under the assumption that spacetime is approximately flat, all kinds of terms need to be computed to obtain corrections to the propagator [44] [45]. I will construct the propagator differently, under the assumption that a solution to the homogeneous Dirac equation of motion is at hand. The propagator can then be constructed by multiplying two such solutions $D(r, r', \Omega, k) \sim \psi(r_<)\tilde{\psi}(r_>) + \psi(r_>)\tilde{\psi}(r_<)$ (see also [46]). Here the radial coordinates are written as $r_<$, $r_>$ to indicate which one is closer to the horizon or boundary.
There are two boundary conditions we need to impose. First of all the $\psi(r_<)$ part of $D(r, r')$ should be chosen such that near the horizon it represents an infalling solution, i.e. $\psi(r_<) = \psi_{in}(r_<)$. This is due to the demanded causality, which prohibits fields to pop up out of the horizon. An infalling solution represents a situation that happens, rather than something that "unhappens". Secondly, near the boundary the Green's function should be normalizable, we therefore choose $\psi(r_>) = \psi_n(r_>)$.

Claim
The fermionic bulk-to-bulk propagator, the solution to equation 6.7, is given by

$$\boxed{D(r, r', \Omega, k) = G_R(\Omega, k)\begin{cases}\psi^{in}(r)\tilde{\psi}^n(r') & r < r' \\ \psi^n(r)\tilde{\psi}^{in}(r') & r > r'\end{cases}}, \tag{6.8}$$

where boundary conditions are implemented in the way which was described above, and where $\tilde{\psi} \equiv \psi^T\Gamma^0 = i\psi^T\sigma_1$ is defined.
This claim is insensitive to the precise metric we choose and will therefore have general applicability.

Proof
The term $G_R(\Omega, k)$ in front of the above expression will naturally arise after plugging in the rest of the expression into the Green's function, [2]

$$\begin{aligned}\Big(\not{D} - m\Big)G(r, r') =& \Big[e^r{}_{\bar{r}}\Gamma^{\bar{r}}\partial_r - m\Big]\Big(\Theta(r' - r)\psi^{in}(r)\tilde{\psi}^n(r') + \Theta(r - r')\psi^n(r)\tilde{\psi}^{in}(r')\Big) \\ =& e^r{}_{\underline{r}}\Gamma^{\underline{r}}\delta(r' - r)\psi^{in}(r)\tilde{\psi}^n(r') + \Theta(r' - r)e^r{}_{\underline{r}}\Gamma^{\underline{r}}(\partial_r\psi^{in}(r))\tilde{\psi}^n(r') \\ &+ e^r{}_{\underline{r}}\Gamma^{\underline{r}}\delta(r - r')\psi^n(r)\tilde{\psi}^{in}(r') + \Theta(r - r')e^r{}_{\underline{r}}\Gamma^{\underline{r}}(\partial_r\psi^n(r))\tilde{\psi}^{in}(r') \\ &- m\Big(\Theta(r' - r)\psi^{in}(r)\tilde{\psi}^n(r') + \Theta(r - r')\psi^n(r)\tilde{\psi}^{in}(r')\Big).\end{aligned} \tag{6.9}$$

[2] Another route uses two forms of the Green's function; the Green's function equation at $r \neq r'$, and an integrated version of the form $\int_{r=r'-\epsilon}^{r=r'+\epsilon} \Box\psi = 1$, thanks to Sean Hartnoll for pointing this out.

Use the assumption that ψ is a solution to the Dirac equation to rewrite the second and fourth term,

$$\begin{aligned}\Big(\not{D}-m\Big)G(r,r') =& -\sqrt{g^{rr}}\sigma_3\delta(r'-r)\psi^{in}(r)\tilde{\psi}^n(r') + \cancel{\Theta(r'-r)m\psi^{in}(r)\tilde{\psi}^n(r')} \\ &+\sqrt{g^{rr}}\sigma_3\delta(r-r')\psi^n(r)\tilde{\psi}^{in}(r') + \cancel{\Theta(r-r')m\psi^n(r)\tilde{\psi}^{in}(r')} \\ &-m\Big(\cancel{\Theta(r'-r)\psi^{in}(r)\tilde{\psi}^n(r')} + \cancel{\Theta(r-r')\psi^n(r)\tilde{\psi}^{in}(r')}\Big) \\ =&\delta(r-r')\sqrt{g^{rr}}\Big(\sigma_3\psi^n(r)\tilde{\psi}^{in}(r') - \sigma_3\psi^{in}(r)\tilde{\psi}^n(r')\Big). \end{aligned} \tag{6.10}$$

The radial arguments can be dropped because the normalization is only needed if $r = r'$ anyway. Writing out in spinor components,

$$\begin{aligned}\Big(\not{D}-m\Big)G(r,r') &= \delta(r-r')\sqrt{g^{rr}}i\Big(\sigma_3\psi^n(\psi^{in})^T\sigma_1 - \sigma_3\psi^{in}(\psi^n)^T\sigma_1\Big) \\ &= \delta(r-r')\sqrt{g^{rr}}i\Big[\begin{pmatrix}\psi_1^n\\-\psi_2^n\end{pmatrix}(\psi_2^{in},\psi_1^{in}) - \begin{pmatrix}\psi_1^{in}\\-\psi_2^{in}\end{pmatrix}(\psi_2^n,\psi_1^n)\Big] \\ &= \delta(r-r')\sqrt{g^{rr}}i\begin{pmatrix}\psi_1^n\psi_2^{in}-\psi_1^{in}\psi_2^n & 0\\ 0 & \psi_2^{in}\psi_1^n-\psi_2^n\psi_1^{in}\end{pmatrix} \\ &= \frac{\delta(r-r')}{\sqrt{-g}}\sqrt{-g}\sqrt{g^{rr}}i\Big(\psi_1^n\psi_2^{in}-\psi_1^{in}\psi_2^n\Big)\mathbb{1}_{2\times2}, \end{aligned} \tag{6.11}$$

we see that we can normalize the solution with a Wronskian

$$\begin{aligned}W(\psi^n,\psi^{in}) &\equiv \sqrt{-g}\sqrt{g^{rr}}(\tilde{\psi}^{in}\sigma_3\psi^n - \tilde{\psi}^n\sigma_3\psi^{in}) \\ &= \sqrt{-g}\sqrt{g^{rr}}((\psi^{in})^T i\sigma_1\sigma_3\psi^n - (\psi^n)^T i\sigma_1\sigma_3\psi^{in}) \\ &= \sqrt{-g}\sqrt{g^{rr}}((\psi^{in})^T\sigma_2\psi^n - (\psi^n)^T\sigma_2\psi^{in}) \\ &= \sqrt{-g}\sqrt{g^{rr}}i\Big(\psi_1^n\psi_2^{in}-\psi_1^{in}\psi_2^n\Big)\mathbb{1}_{2\times2}. \end{aligned} \tag{6.12}$$

To calculate what this object is, recall from 5.17 the form of the solution near the boundary,

$$\psi(r) \overset{r\to\infty}{\longrightarrow} \psi^- r^{-1-m}\begin{pmatrix}0\\1\end{pmatrix} + \psi^+ r^{-1+m}\begin{pmatrix}1\\0\end{pmatrix}. \tag{6.13}$$

whose normalizable part at the boundary is the first term $\psi^n \sim r^{-1-m}\begin{pmatrix}0\\1\end{pmatrix}$.

We can also write the infalling solution ψ^{in} as a linear combination of a part ψ^n which is normalizable near the boundary, and a part $\psi^{n.n.}$ which is non-normalizable,

$$\begin{aligned}\psi^{in}(r_<) &= \psi^{n.n.}(r_<,\omega,k) + G^R(\omega,k)\psi^n(r_<,\omega,k) \\ &\sim r^{-1-m}\begin{pmatrix}0\\1\end{pmatrix} + \frac{1}{G_R}r^{-1+m}\begin{pmatrix}1\\0\end{pmatrix}. \end{aligned} \tag{6.14}$$

In this expression appears the boundary retarded Green's function as the proportionality between the two independent modes. This is due to the *definition* of the retarded Green's function being the ratio of the

pre-factors of normalizable and non-normalizable solutions, with the additional demand that the solution should be infalling at the horizon to ensure causality.
One might wonder why we impose that normalizability constraint on the spinor $\psi(r_>)$ if there is still a non normalizable part to $\psi_{in}(r_<)$. Because you can never take both r and r' in equation 6.8 to the boundary simultaneously, $\psi_{in}(r)$ is never strictly 'near' the boundary. In other words, one of them is always smaller and therefore *not* on the boundary. Writing out the Wronskian,

$$\begin{aligned} W(\psi^n,\psi^{in}) &= \sqrt{-g}\sqrt{g^{rr}}(\tilde{\psi}^{in}\sigma_3\psi^n - \tilde{\psi}^n\sigma_3\psi^{in}) \\ &= \frac{ir^2}{L^2}\left[\left(G_R^{-1}r^{m-1}, r^{-1-m}\right)\begin{pmatrix}0 & -1\\ 1 & 0\end{pmatrix}\begin{pmatrix}0\\ r^{-1-m}\end{pmatrix} - \left(0, r^{-1-m}\right)\begin{pmatrix}0 & -1\\ 1 & 0\end{pmatrix}\begin{pmatrix}\frac{1}{G_R}r^{m-1}\\ r^{-1-m}\end{pmatrix}\right] \\ &= \frac{2iL^2}{G_R}, \end{aligned} \tag{6.15}$$

and combining equations 6.11 6.12 6.15 it is evident that the claim in 6.8 is justified.[3]

6.2 Effective vertices

Using the result of the previous section and putting all these pieces together into a Wick rotated equation 6.5 gives

$$\begin{aligned} \tilde{\chi}(\omega,q) =& \frac{(iq)^2}{2}\int dr\sqrt{g}\,dr'\sqrt{g'}\int\frac{d\Omega}{2\pi}\int\frac{dk}{2\pi}A_t(r)A_t(r') \\ & \mathrm{Tr}\Big[\Theta(r-r')\Gamma^t G_R(\Omega,k)\psi^n(r)\tilde{\psi}^{in}(r')\Gamma^t G_R(\Omega+\omega,k+q)\psi^{in}(r')\tilde{\psi}^n(r) \\ & + \Theta(r'-r)\Gamma^t G_R(\Omega,k)\psi^{in}(r)\tilde{\psi}^n(r')\Gamma^t G_R(\Omega+\omega,k+q)\psi^n(r')\tilde{\psi}^{in}(r)\Big], \end{aligned} \tag{6.16}$$

where the two possibilities $r>r', r<r'$ where treated separately. Interchanging $r\leftrightarrow r'$ in the second term

$$\begin{aligned} \tilde{\chi}(\omega,q) =& \frac{(iq)^2}{2}\int dr\sqrt{g}\,dr'\sqrt{g'}\int\frac{d\Omega}{2\pi}\int\frac{dk}{2\pi}A_t(r)A_t(r')G_R(\Omega,k)G_R(\Omega+\omega,k+q)\Theta(r-r') \\ & \mathrm{Tr}\Big[\Gamma^t\psi^n(r)\tilde{\psi}^{in}(r')\Gamma^t\psi^{in}(r')\tilde{\psi}^n(r) + \Gamma^t\psi^{in}(r')\tilde{\psi}^n(r)\Gamma^t\psi^n(r)\tilde{\psi}^{in}(r')\Big], \end{aligned} \tag{6.17}$$

and using the cyclic property of the trace,

$$\begin{aligned} \tilde{\chi}(\omega,q) =& (iq)^2\int dr\sqrt{g}\,dr'\sqrt{g'}\int\frac{d\Omega}{2\pi}\int\frac{dk}{2\pi}A_t(r)A_t(r')G_R(\Omega,k)G_R(\Omega+\omega,k+q)\Theta(r-r') \\ & \mathrm{Tr}\Big[\tilde{\psi}^n(r)\Gamma^t\psi^n(r)\tilde{\psi}^{in}(r')\Gamma^t\psi^{in}(r')\Big]. \end{aligned} \tag{6.18}$$

The argument of the trace is a scalar so Tr can be dropped. Further note that the (r,r')-dependence of this expression appears exclusively in the wave functions, and that these terms factorize in terms depending on

[3] This is up to a factor 2 which can be absorbed into the definition of the Wronskian.

r and terms depending on r',

$$\tilde{\chi}(i\omega,q) =(iq)^2 \int \frac{d\Omega}{2\pi} \int \frac{dk}{2\pi} G_R(\Omega,k)G_R(\Omega+\omega,k+q) \\ \int_0^{\Upsilon} dr' \sqrt{g'}\sqrt{g'} A_t(r')\tilde{\psi}^{in}(r')e^t_{\underline{t}}\Gamma^{\underline{t}}\psi^{in}(r') \int_{\Upsilon}^{\infty} dr\sqrt{g}A_t(r)\tilde{\psi}^{n}(r)e^t_{\underline{t}}\Gamma^{\underline{t}}\psi^{n}(r), \tag{6.19}$$

where Υ is as a cutoff on the radial integral which arises due to the Heaviside step function in 6.18, and where the vielbeins where introduced because the gamma matrices are only defined in flat space.
The next subsections will show that these radial integrals don't diverge and can be denoted by *effective vertices* Λ (for a similar calculation, see [47]). In order to investigate possible divergencies we need to consider the radial integrals in the different regions of the BTZ spacetime. Recall that at $T = 0$, the near horizon region has an $AdS_2 \times \mathbb{R}$ geometry $ds^2 = \frac{-d\tau^2+d\zeta^2}{\zeta^2} + dx^2$. In this region the equation of motion for

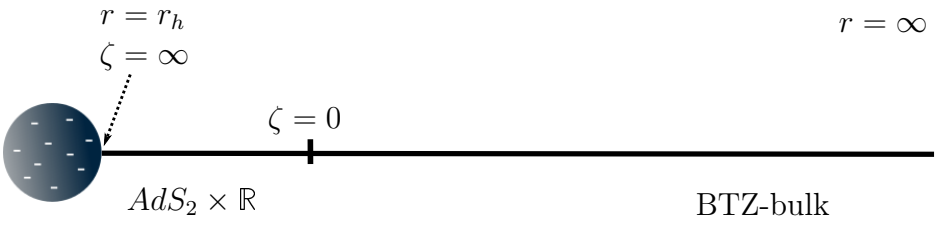

Figure 6.2: Various regions of spacetime.

the upper component of the fermionic field with infalling boundary conditions is solved by equation 5.36,

$$\psi_1(\zeta) = B_1 e^{i\omega\zeta}(-2i\omega\zeta)^{\nu+\frac{1}{2}} U(\nu - iq\rho + 1, 1 + 2\nu; -2i\omega\zeta), \tag{6.20}$$

while the lower component reads [4]

$$\psi_2(\zeta) = B_2 e^{i\omega\zeta}(-2i\omega\zeta)^{\nu+\frac{1}{2}} U(\nu - iq\rho, 1 + 2\nu; -2i\omega\zeta). \tag{6.21}$$

Note that the radial coordinate $\zeta = \frac{L_2^2}{r-r_h}$ for the near the horizon appears always multiplied with ω. In the near horizon region therefore also $\zeta\omega$ can be used to denote the radial position.

6.2.1 Near horizon: $\zeta\omega \gg 1$

To find the near horizon behavior of the solutions 6.23, 6.21 use the identity

$$U(a,b,x) \overset{x\to\infty}{\sim} x^{-a}{}_2F_0(a, a-b+1; \ ; -1/x). \tag{6.22}$$

[4]The extra minus sign mentioned in equation 5.29 means that the infalling solution is $W_{\frac{1}{2}+iq\rho,\nu}(-2i\omega\zeta)$. To find equation 6.21 once again use 5.35.

As a result near the horizon the solutions have the form

$$\begin{aligned}\psi_1(\zeta\to\infty) &= B_1 e^{i\omega\zeta}(-2i\omega\zeta)^{\nu+\frac{1}{2}}(-2i\omega\zeta)^{-\nu+iq\rho-1}\,{}_2F_0(\nu-iq\rho+1,-iq\rho-\nu;\ ;-1/2i\omega\zeta)\\ &\sim e^{i\omega\zeta}\zeta^{iq\rho-\frac{1}{2}}\\ \psi_2(\zeta\to\infty) &= B_2 e^{i\omega\zeta}(-2i\omega\zeta)^{\nu+\frac{1}{2}}(-2i\omega\zeta)^{-\nu+iq\rho}\,{}_2F_0(\nu-iq\rho,-\nu-iq\rho-1;\ ;-1/2i\omega\zeta)\\ &\sim e^{i\omega\zeta}\zeta^{iq\rho+\frac{1}{2}}.\end{aligned} \tag{6.23}$$

The measure of the radial integral in the near horizon region is rewritten in terms of ζ,

$$\begin{aligned}\int dr\sqrt{-\det g_{\mu\nu}(r)} &= \int \frac{dr}{d\zeta}d\zeta\sqrt{-\det\frac{d\zeta^\alpha}{dr^\mu}\frac{d\zeta^\beta}{dr^\nu}g_{\alpha\beta}(\zeta)}\\ &= \int \frac{dr}{\cancel{d\zeta}}\frac{\cancel{d\zeta}}{dr}d\zeta\sqrt{-\det g_{\alpha\beta}(\zeta)}\\ &= \int\frac{d\zeta}{\zeta^2}.\end{aligned} \tag{6.24}$$

Recall that $\tilde{\psi}=\psi^T\Gamma^{\underline{t}}$ and that the gauge field in the near horizon region ($\zeta\gg 1$) reads $A_t(\zeta)\sim\frac{1}{\zeta}$. The vielbein in this region is given by $e^t{}_{\underline{t}}=\zeta$. The contribution to the effective vertex of the near horizon region can now be calculated,

$$\begin{aligned}\Lambda_{nearhorizon} &\sim \int_{cutoff}^{\infty}\frac{d\zeta}{\zeta^2}A_t(\psi^{in})^T e^t{}_{\underline{t}}(\Gamma^{\underline{t}})^2\psi^{in}\\ &= -\int_{cutoff}^{\infty}\frac{d\zeta}{\zeta^2}\frac{1}{\zeta}\zeta\Big(\psi_1^2+\psi_2^2\Big)\\ &= -\int_{cutoff}^{\infty}\frac{d\zeta}{\zeta^2}\Big(\frac{1}{\zeta}+\zeta\Big)e^{2i\omega\zeta}\zeta^{2iq\rho}\sim\zeta^{2iq\rho}<\infty.\end{aligned} \tag{6.25}$$

For finite charge this region does not give rise to divergencies.

6.2.2 The boundary of the near horizon $AdS_2\times\mathbb{R}$ region: $\zeta\omega\ll 1$

Other possible divergencies might arise at the boundary of the $AdS_2\times\mathbb{R}$ where the radial coordinate $\zeta\omega\ll 1$. Near this boundary the spinor solution is of the form

$$\Psi(\zeta)=\psi_+\zeta^{\frac{1}{2}+\nu}+\psi_-\zeta^{\frac{1}{2}-\nu}\qquad\qquad \nu=\sqrt{m^2+k^2-(q\rho)^2}, \tag{6.26}$$

such that the normalizable part is given by $\psi(\zeta)\sim\zeta^{\frac{1}{2}+\nu}$. The vertex contribution is

$$\Lambda_{\partial AdS_2}=\int_0^{cutoff}\frac{d\zeta}{\zeta^2}A_t(\zeta)e^t{}_{\underline{t}}\big(\zeta^{\frac{1}{2}+\nu}\big)^2=\int_0^{cutoff}d\zeta\zeta^{-1+2\nu}\sim\zeta^{2\nu}, \tag{6.27}$$

which is finite for $\nu>0$.

6.2.3 UV: bulk $AdS_3 - BTZ$

Near the asymptotic AdS boundary of the full BTZ geometry the normalizable spinor of equation 5.17 scales as $\psi_n(r) = r^{-1-m}$. In this region the vielbein has the value $e^t{}_{\underline{t}} = \sqrt{-g^{tt}} \overset{r\to\infty}{\sim} \frac{1}{r}$. The effective vertex gets a contribution

$$\begin{aligned}\Lambda_{boundary} &= \int_{cutoff}^{\infty} dr\ \sqrt{-g} A_t(r) \tilde{\psi}_n e^t{}_{\underline{t}} \Gamma^{\underline{t}}(r) \psi_n(r) \\ &= \int_{cutoff}^{\infty} dr\ r^{-2-2m} \log r \\ &\sim -\frac{1}{r^{2m-1}}(1 + 2m \log r)\Big|_{r=cutoff}^{r=\infty},\end{aligned} \tag{6.28}$$

which is finite if $m > -\frac{1}{2}$. We conclude that this region cannot cause divergencies in the effective vertices.

Conclusion: the effective vertex integrals are finite.

They will be denoted by the letter Λ in which also a factor of iq is absorbed. The density susceptibility 6.19 now reads

$$\tilde{\chi}(\omega, q) = \Lambda^2 \int \frac{d\Omega}{2\pi} \int \frac{dk}{2\pi} G_R(\Omega, k) G_R(\Omega + \omega, k + q), \tag{6.29}$$

It was argued in section 5.3 that near the Fermi surface the Green's functions have the form

$$G_{l,r}(k, \omega) = \frac{1}{\pm k - k_f - \frac{1}{v_f}\omega - c\omega^{2\nu_k}}, \tag{6.30}$$

with c a complex number. The subscript r, l makes a distinction between the two Fermi points. The $q = 2k_f$ behavior we are interested in arises when the arguments of both Green's function are at either one of $k \approx \pm k_f$, $\omega \approx 0$. This is satisfied with the combination $k + q - k_f = 0$ and $-k - k_f = 0$. Because with this choice of arguments both Green's functions are close to the Fermi surface (where the Green's function are singular), the integral obtains its major contribution in this region.
We seem to end up in a situation where we will always have results which depend on ν_k, associated with the near horizon region of the BTZ geometry. This is in agreement with the picture of holographic renormalization where it is argued that low energies of the dual field theory are to be associated with the deep interior of the bulk, as was argued in section 3.4.
The above result 6.29 is to be compared with 2.4. The remarkable observation that we make at this point is that the computation in AdS comes down to the same integral as calculated in chapter 2. The only difference lies in the near horizon Green's function which shows up as the self-energy, giving a nontrivial $\Sigma \sim \omega^{2\nu_k}$ scaling.

The the remaining integrals cannot be calculated analytically. The next subsection assumes a k-independent ν, in which case analytic statements *are* possible.

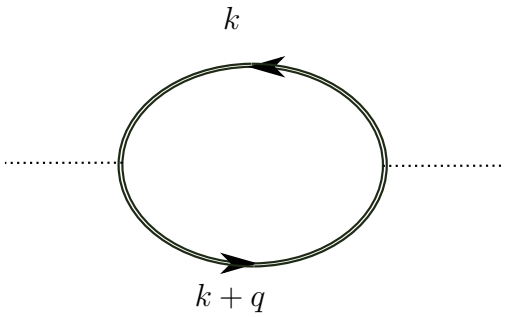

Figure 6.3: Particle-hole bubble contributing to the density susceptibility. Compared to the calculation done in section 2.2, the single particle propagators are replaced by Green's functions with a nontrivial self-energy which arises from the near BTZ horizon IR Green's function.

6.3 Analytic results

The real space density-density correlation function is given by the Fourier transform of the density susceptibility. In general for k dependent ν_k our integrals are not solvable with analytic techniques. If, however, we assume for the moment that ν_k is k-independent, which is true near the Fermi surface where the integral obtains its major contribution, there is an analytic result possible.[5]

Taking the aforementioned Fourier transform of the result obtained in 6.29 gives the real space density correlation function, [6]

$$\begin{aligned}
\chi(x,t=0) &= \int dq \int d\omega \tilde{\chi}(q,\omega) e^{iqx} e^{-i\omega t} \\
&= \int dq \int d\omega \Big[\int dk \int d\Omega \;\; G_l(\Omega+\omega, k+q) G_r(\Omega,k) \Big] e^{iqx} e^{-i\omega t} \\
&= \int dk \int d\Omega \Big(\int dq \int d\omega \;\; G_l(\Omega+\omega, k+q) e^{iqx} e^{-i\omega t} \Big) G_r(\Omega,k) \\
&= \int dk \int d\Omega \Big(\int dq \int d\omega \;\; G_l(\omega,q) e^{i(q-k)x} e^{-i(\omega-\Omega)t} \Big) G_r(\Omega,k) \\
&= \int dq \int d\omega \;\; G_l(\omega,q) e^{iqx} \cancel{e^{-i\omega t}} \int dk \int d\Omega \;\; G_r(\Omega,k) e^{-ikx} \cancel{e^{i\Omega t}}.
\end{aligned} \tag{6.31}$$

Notice the similarity between the proof of the convolution theorem $\mathcal{F}\{f * g\} = \mathcal{F}\{f\}\mathcal{F}\{g\}$ and the above calculation.

Since we are interested in the $k \approx k_f$, $\omega \approx 0$ regime, the value of ν determines which ω-dependent term in equation 6.30 is more important. We restrict to the interesting $\nu < \frac{1}{2}$ regime (the $\nu > \frac{1}{2}$ will give back the familiar fermi liquid like behavior, as I discuss in the end). This means that the term linear in ω is dropped

[5] I thank Subir Sachdev for pointing this out to me.

[6] The exponential $e^{-i\omega t}$ associated with the ω integral was added to make it more transparent, but keep in mind that in the end $t = 0$.

because it vanishes faster near $\omega \approx 0$. Working out the left moving term of equation 6.31,

$$\begin{aligned}
\int dq \int d\omega \;\; G_l(\omega, q) e^{iqx} \quad &= \quad \int dq \int d\omega \;\; \frac{1}{q - k_f - c\omega^{2\nu}} e^{iqx} \\
&\overset{q \to q + k_f}{=} \quad e^{ik_f x} \int dq \int d\omega \;\; \frac{1}{q - c\omega^{2\nu}} e^{iqx} \\
&\overset{\tilde{q} = qx}{=} \quad e^{ik_f x} \frac{1}{x} \int d\tilde{q} \int d\omega \;\; \frac{x}{\tilde{q} - c\omega^{2\nu} x} e^{i\tilde{q}} \\
&\overset{\tilde{\omega} = \omega x^{1/2\nu}}{=} \quad e^{ik_f x} x^{-\frac{1}{2\nu}} \int d\tilde{q} \int d\tilde{\omega} \;\; \frac{1}{\tilde{q} - c\tilde{\omega}^{2\nu}} e^{i\tilde{q}} \\
&\sim \quad e^{ik_f x} x^{-\frac{1}{2\nu}}.
\end{aligned} \tag{6.32}$$

Likewise for the right mover,

$$\begin{aligned}
\int dq \int d\omega \;\; \mathcal{G}_r(\omega, q) e^{-ikx} \quad &= \quad \int dq \int d\omega \;\; \frac{1}{-k - k_f - c\omega^{2\nu}} e^{-ikx} \\
&\overset{k \to k - k_f}{=} \quad e^{ik_f x} \int dq \int d\omega \;\; \frac{1}{-k - c\omega^{2\nu}} e^{-ikx} \\
&\sim \quad e^{ik_f x} x^{-\frac{1}{2\nu}}.
\end{aligned} \tag{6.33}$$

This leads to a contribution to the real space density-density correlation function

$$\boxed{\chi(x, t = 0) = e^{2ik_f x} x^{-\frac{1}{\nu}} \qquad \nu < \frac{1}{2}}. \tag{6.34}$$

What does $\nu < \frac{1}{2}$ mean? Lets recall the definition $\nu_k = \sqrt{m^2 + k^2 - (q\rho)^2}$. Since we have $k \approx k_f$,

$$\nu < \frac{1}{2} \qquad \Rightarrow m^2 + k_f^2 - (q\rho)^2 < \frac{1}{4}. \tag{6.35}$$

The mass/charge ratio 6.35 sets the threshold for the possibility of scaling with special power law behavior.

The special scaling at $q = 2k_f$ we find is certainly interesting. The question remains however if the field theory we describe holographically is in any way related to the Luttinger liquid, or that our result is just coincidental.

The case $\nu \geq \frac{1}{2}$ means that the linear term in the Green's function 6.30 dominates around $\omega \approx 0$. We can use our current result 6.34 and fill in "ν"$= \frac{1}{2}$, leading to x^{-2} scaling, just like in Fermi liquid theory.[7] This is an indication that our result should be doubted.

[7] Quotation marks emphasize that in this case ν is not the conformal dimension, but just the power with which the dominant ω-term scales.

Chapter 7

Conclusion and Discussion

Quantum corrections to a gauge field propagator in a BTZ black hole background were studied. These 1/N suppressed processes were shown to be a possible cause of the anomalous scaling of the density two-point function in the holographic description of low-dimensional fermions.

To come to this conclusion, first low-dimensional interacting fermion systems were studied in chapter 2. Fermi liquid theory was presented and in particular its inability to describe interacting electrons in one spatial dimension. A derivation was presented of the interaction dependent scaling of the Luttinger model in the density two point function at $2k_f$. This scaling traces back to perfect nesting in one dimension at that wave vector causing a logarithmic divergence in the particle-hole channel.

Chapter 3 introduced the basic principles of the AdS/CFT correspondence and in particular its application to condensed matter. Because AdS/CFT is a *holographic* correspondence, the dual gravitational description of interacting fermions in two spacetime dimensions must have a three dimensional negatively curved metric. The BTZ black hole was presented in chapter 4 as the best candidate to start this holographic computation. In this chapter we derived the charged BTZ black hole as the unique black hole solution with negative cosmological constant and non-vanishing electric field on the boundary. We further showed that the near horizon region of the extremal BTZ black hole has an emergent $\mathrm{AdS}_2 \times \mathbb{R}$ geometry, similar to the near horizon region of the Reisner-Nordröm black hole.

In chapter 5, we introduced fermions in the BTZ background and analyzed the Dirac equation for various regions of spacetime. Here we showed that the spin connection can be removed in the same manner as was known for higher-dimensional black holes. In the near horizon geometry the Dirac equation was solved exactly. We thereby re-derived a result known in the literature for the specific case of a BTZ black hole. The boundary retarded Green's function was constructed by matching solutions of the inner and outer spacetime regions. In a certain regime of the parameters this Green's function takes a familiar form with a self-energy term whose scaling depends on the conformal dimension of an operator on the boundary of the near horizon region.

In chapter 6, we moved away from the large N limit by investigating a 1/N suppressed fermionic loop correction to the gauge field propagator which arises in a second order expansion in the electromagnetic coupling. In the loop diagram appeared bulk-to-bulk fermion propagators which were constructed by multiplying two spinor solutions of the homogeneous Green's function equation. The resulting loop amplitude factorized in terms at different radial coordinates. These so-called effective vertices were shown not to diverge in any

region of the BTZ geometry. Interestingly, the remaining part of the loop amplitude had a form similar to the expression found in the field theory calculation done in the second chapter. The effective vertices put aside, all information on the extra dimension of AdS was captured in the non-trivial IR scaling of the self-energy of the boundary Green's functions. The resulting integrals could be solved analytically under the simplification that these IR conformal dimension are constant, which is largely true near the Fermi surface, where the integral obtains its major contribution. In a certain regime of parameters we found special scaling in the gauge field two-point function at $q = 2k_f$. Although this scaling is certainly interesting, the question remains if the field theory we hereby describe holographically is indeed really a Luttinger liquid.

Appendix A

Linear Response

An important tool in physics is the theory of linear response.[1] It provides a bridge between theoretical predictions on one side and experiments on the other. Linear response describes how a system in thermal equilibrium reacts to a perturbation by an external, time dependent force $F(t,x)$. This force couples to an operator of the system and thereby introduces a perturbation term (switched on adiabatically at $t=-\infty$) to the Hamiltonian,

$$\hat{H} = \hat{H}_0 + \int d^d x F(x,t)\hat{X}. \tag{A.1}$$

For small driving forces this reaction is supposed to be linear,

$$X = \int d^d x \int dt \chi_{ij}(x,x',t,t')F(x,t). \tag{A.2}$$

The function χ, the response function (or susceptibility) is a property of the system. It measures the response of expectation value of some operator of the system to some applied perturbation. A few observations can be made on general grounds:
The system cannot react to any forces which have not been applied yet. Put differently, the response function is retarded $\chi_{ij}(x,x',t,t') = \Theta(t-t')\chi_{ij}(x,x',t,t')$.
Secondly, if the original Hamiltonian does not depend on time, the response function will depend only on time differences $t-t'$, $\chi_{ij}(x,x',t,t') = \chi_{ij}(x,x',t-t')$.
If the system is spatially translation invariant the response function only depends on spatial distances $x-x'$, $\chi_{ij}(x,x',t,t') = \chi_{ij}(x-x',t,t')$.

[1] In this section I use the notation of Altland and Simons [48].

A.1 Microscopic considerations

The expectation value of some operator can be written using bosonic or fermionic functions,

$$\langle \hat{X} \rangle = \sum_{\alpha\alpha'} \langle \bar{\psi}_\alpha X_{\alpha\alpha'} \psi_{\alpha'} \rangle. \tag{A.3}$$

To calculate the expectation value, a functional integral, one needs to specify the action,

$$\begin{aligned} S[F, F'\bar{\psi}, \psi] &= S_0[\bar{\psi}, \psi] + \delta S[F, \bar{\psi}, \psi] + \delta S'[F', \bar{\psi}, \psi] \\ &= S_0[\bar{\psi}, \psi] + \int d\tau F(\tau) \sum_{aa'} \bar{\psi}_a(\tau) X_{aa'} \psi_{a'}(\tau) + \int d\tau F'(\tau) \sum_{aa'} \bar{\psi}_a(\tau) X'_{aa'} \psi_{a'}(\tau), \end{aligned} \tag{A.4}$$

which is also used to find the partition function $\mathcal{Z}$.
Taking functional derivatives

$$\begin{aligned} \langle \hat{X} \rangle &= -\mathcal{Z}^{-1} \frac{\delta}{\delta F(\tau)} \Big|_{F=0} \ln \mathcal{Z}[F, F'] \\ &\approx -\int d\tau' \left[\frac{\delta^2}{\delta F(\tau) \delta F'(\tau')} \Big|_{F=F'=0} \ln \mathcal{Z}[F, F'] \right] F'(\tau'), \end{aligned} \tag{A.5}$$

and comparing this to A.2 gives

$$\chi_{ij}(\tau, \tau') = -\mathcal{Z}^{-1} \frac{\delta^2}{\delta F(\tau) \delta F'(\tau')} \Big|_{F=F'=0} \mathcal{Z}[F, F']. \tag{A.6}$$

A.1.1 The plethora of real-time response function

The path integral approach to field theory naturally delivers us with the imaginary time (Euclidean) correlation function

$$C^{\tau}_{X_1 X_2}(\tau_1 - \tau_2) = -\langle T_\tau \hat{X}_1(\tau_1) \hat{X}_2(\tau_2) \rangle. \tag{A.7}$$

We are interested however response $\chi(x, x', t, t')$ of the system in the real time to a real time perturbation $F(x, t)$. We can define three different response functions.; the real time response function

$$C^{t}_{X_1 X_2}(t_1 - t_2) = -i\langle T_t \hat{X}_1(t_1) \hat{X}_2(t_2) \rangle, \tag{A.8}$$

the retarded response function

$$C^{+}_{X_1 X_2}(t_1 - t_2) = -i\Theta(t_1 - t_2) \langle [\hat{X}_1(t_1), \hat{X}_2(t_2)]_{\zeta_X} \rangle, \tag{A.9}$$

and the advanced response function

$$C^{-}_{X_1 X_2}(t_1 - t_2) = i\Theta(t_2 - t_1) \langle [\hat{X}_1(t_1), \hat{X}_2(t_2)]_{\zeta_X} \rangle, \tag{A.10}$$

where $\zeta_X = 1$ for bosons and $\zeta_X = -1$ for fermions. The retarded time response functions turns out to be most important one. This is because this one generates the linear response of $\hat{X}$ to the presence of a perturbation.
Using the Lehman representation, which expresses the correlation functions in terms of eigenvalues of a complete set of eigenfunctions, the different response functions can be connected. If, for example, one has an explicit expression for $C^{\tau}_{X_1X_2}(\tau_1-\tau_2)$, we can obtain $C^{+}_{X_1X_2}(t_1-t_2)$ by a Wick rotation $i\omega \to \omega+i\delta$. This infinitesimally small δ makes sure no branch cuts are crossed. Also it has a very physical interpretation: it makes sure that the perturbation is turned on *adiabatically* at $t = -\infty$. The poles of the retarded correlation function all lie in the lower half of the complex plane. A pole in the upper half plane would lead to a mode that is growing in time and is therefore non-normalizable.

A.2 The spectral function

The *spectral function* is introduced as

$$A(\omega) \equiv -2\mathrm{Im}C^{+}(\omega). \tag{A.11}$$

The retarded and the advanced correlation functions are related through complex conjugation $C^{+}(\omega) = [C^{-}(\omega)]^{*}$.[2] It follows that $\mathrm{Im}C^{+}(\omega) = -\mathrm{Im}C^{-}(\omega)$, and consequently,

$$A(\omega) = i(C^{+}(\omega) - C^{-}(\omega)). \tag{A.12}$$

The spectral function contains the same amount of information as the correlation function itself,

$$\int_{-\infty}^{\infty} \frac{d\omega}{2\pi} \frac{A(\omega)}{z-\omega} = \int_{-\infty}^{\infty} \frac{d\omega}{2\pi} \frac{i(C^{+}(\omega) - C^{-}(\omega))}{z-\omega} = C(z). \tag{A.13}$$

This complex integral is computed after recognition of the fact that $C^{+}(\omega)(C^{-}(\omega))$ only has poles in the upper (lower) imaginary plane. These poles coincide with those of $C(z)$.
The physical meaning of the spectral function becomes apparent if we look at the Fermi gas (non-interacting fermions). Wick rotating the single particle propagator to $G_R(k, i\omega \to \omega + i\delta) = \frac{1}{p_\perp - \omega - i\delta}$ and using $\lim_{\eta\to 0} \frac{1}{x \pm i\eta} = \mp i\pi\delta(x) + \mathcal{P}\frac{1}{x}$ we see that the spectral function of a Fermi gas,

$$\mathrm{Im}G_R(\omega) = \delta(p_\perp - \omega), \tag{A.14}$$

has a single peak at the particle energy. The spectral function is therefore a measure of the probability to find a excitation with a specific energy.[3] In the case of the interacting Fermi gas (Fermi liquid) $G_p(\omega) = \frac{1}{p_\perp - \omega + \Sigma}$ this delta function peak is smeared out to a Lorentzian profile,

$$A(\omega) = \frac{\mathrm{Im}\Sigma}{(k_\perp^2 - \omega + \mathrm{Re}\Sigma)^2 + \mathrm{Im}\Sigma^2}. \tag{A.15}$$

[2] This can be derived easily using the Lehman representation.
[3] Probabilities are normalized because $\int \frac{d\omega}{2\pi} A_\alpha(\omega) = 1$.

Appendix B

Curvature and the Einstein Equation

From a given metric $g_{\alpha\beta}$, this *Mathematica* notebook computes the components of the following: the inverse metric, $g^{\lambda\sigma}$, the Christoffel symbols or affine connection, [1]

$\Gamma^{\lambda}{}_{\mu\nu} = \frac{1}{2} g^{\lambda\sigma} (\partial_\mu g_{\sigma\nu} + \partial_\nu g_{\sigma\mu} - \partial_\sigma g_{\mu\nu})$,

(∂_α stands for the partial derivative $\partial / \partial x^\alpha$), the Riemann tensor,

$R^{\lambda}{}_{\mu\nu\sigma} = \partial_\nu \Gamma^{\lambda}{}_{\mu\sigma} - \partial_\sigma \Gamma^{\lambda}{}_{\mu\nu} + \Gamma^{\eta}{}_{\mu\sigma} \Gamma^{\lambda}{}_{\eta\nu} - \Gamma^{\eta}{}_{\mu\nu} \Gamma^{\lambda}{}_{\eta\sigma}$,

the Ricci tensor

$R_{\mu\nu} = R^{\lambda}{}_{\mu\lambda\nu}$,

the scalar curvature,

$R = g^{\mu\nu} R_{\mu\nu}$,

and the Einstein tensor,

$G_{\mu\nu} = R_{\mu\nu} - \frac{1}{2} g_{\mu\nu} R$.

Clearing the values of symbols:

First clear any values that may already have been assigned to the names of the various objects to be calculated. The names of the coordinates that you will use are also cleared.

Clear[coord, metric, inversemetric, affine, riemann, ricci, scalar, einstein, r, θ, ϕ, t]

Setting the dimension:

The dimension **n** of the spacetime (or space) must be set:

$n = 3$

3

[1] This program was written by *Leonard Parker, University of Wisconsin, Milwaukee* .

Defining a list of coordinates:

```
coord = {r, ϕ, t}
```

$\{r, \phi, t\}$

Defining the BTZ metric:

```
metric = {{(g[r])^(−1), 0, 0}, {0, r^2, 0}, {0, 0, −f[r]}}
```

$\left\{\left\{\frac{1}{g[r]}, 0, 0\right\}, \{0, r^2, 0\}, \{0, 0, -f[r]\}\right\}$

Calculating the inverse metric:

The inverse metric is obtained through matrix inversion.

```
inversemetric = Simplify[Inverse[metric]]
```

$\left\{\{g[r], 0, 0\}, \left\{0, \frac{1}{r^2}, 0\right\}, \left\{0, 0, -\frac{1}{f[r]}\right\}\right\}$

Calculating the Christoffel symbols:

The calculation of the components of the Christoffel symbols is done by transcribing the definition given earlier into the notation of *Mathematica* and using the *Mathematica* functions **D** for taking partial derivatives, **Sum** for summing over repeated indices, **Table** for forming a list of components, and **Simplify** for simplifying the result.

```
affine:=affine = Simplify[Table[(1/2) * Sum[(inversemetric[[i, s]])*
(D[metric[[s, j]], coord[[k]]]+
D[metric[[s, k]], coord[[j]]] − D[metric[[j, k]], coord[[s]]]), {s, 1, n}],
{i, 1, n}, {j, 1, n}, {k, 1, n}]]
```

Displaying the Christoffel symbols:

The nonzero Christoffel symbols are displayed below. You need not follow the details of constructing the functions that we use for that purpose. In the output the symbol Γ[1,2,3] stands for ${\Gamma^1}_{23}$. Because the Christoffel symbols are symmetric under interchange of the last two indices, only the independent components are displayed.

```
listaffine:=Table[If[UnsameQ[affine[[i, j, k]], 0], {ToString[Γ[i, j, k]], affine[[i, j, k]]}],
{i, 1, n}, {j, 1, n}, {k, 1, j}]
```

```
TableForm[Partition[DeleteCases[Flatten[listaffine], Null], 2], TableSpacing → {2, 2}]
```

Γ[1, 1, 1]	$-\frac{g'[r]}{2g[r]}$
Γ[1, 2, 2]	$-rg[r]$
Γ[1, 3, 3]	$\frac{1}{2}g[r]f'[r]$
Γ[2, 2, 1]	$\frac{1}{r}$
Γ[3, 3, 1]	$\frac{f'[r]}{2f[r]}$

Calculating and displaying the Riemann tensor:

The components of the Riemann tensor, $R^{\lambda}{}_{\mu\nu\sigma}$, are calculated using the definition given above.

```
riemann:=riemann = Simplify[Table[
D[affine[[i, j, l]], coord[[k]]] − D[affine[[i, j, k]], coord[[l]]]+
Sum[affine[[s, j, l]]affine[[i, k, s]] − affine[[s, j, k]]affine[[i, l, s]],
{s, 1, n}],
{i, 1, n}, {j, 1, n}, {k, 1, n}, {l, 1, n}]]
```

The nonzero components are displayed by the following functions. In the output, the symbol R[1, 2, 1, 3] stands for $R^1{}_{213}$, and similarly for the other components. You can obtain R[1, 2, 3, 1] from R[1, 2, 1, 3] using the antisymmetry of the Riemann tensor under exchange of the last two indices. The antisymmetry under exchange of the first two indices of $R_{\lambda\mu\nu\sigma}$ is not evident in the output because the components of $R^{\lambda}{}_{\mu\nu\sigma}$ are displayed.

```
listriemann:=Table[If[UnsameQ[riemann[[i, j, k, l]], 0], {ToString[R[i, j, k, l]], riemann[[i, j, k, l]]}],
{i, 1, n}, {j, 1, n}, {k, 1, n}, {l, 1, k − 1}]
```

```
TableForm[Partition[DeleteCases[Flatten[listriemann], Null], 2], TableSpacing → {2, 2}]
```

R[1, 2, 2, 1]	$\frac{1}{2}rg'[r]$
R[1, 3, 3, 1]	$\frac{1}{4}\left(\frac{g[r]f'[r]^2}{f[r]} - f'[r]g'[r] - 2g[r]f''[r]\right)$
R[2, 1, 2, 1]	$-\frac{g'[r]}{2rg[r]}$
R[2, 3, 3, 2]	$-\frac{g[r]f'[r]}{2r}$
R[3, 1, 3, 1]	$\frac{-f[r]f'[r]g'[r]+g[r]\left(f'[r]^2-2f[r]f''[r]\right)}{4f[r]^2g[r]}$
R[3, 2, 3, 2]	$-\frac{rg[r]f'[r]}{2f[r]}$

Calculating and displaying the Ricci tensor:

The Ricci tensor $R_{\mu\nu}$ was defined by summing the first and third indices of the Riemann tensor (which has the first index already raised).

ricci:=ricci = Simplify[Table[Sum[riemann[[i, j, i, l]], {i, 1, n}], {j, 1, n}, {l, 1, n}]]

Next we display the nonzero components. In the output, R[1, 2] denotes R_{12}, and similarly for the other components.

listricci:=Table[If[UnsameQ[ricci[[j, l]], 0], {ToString[R[j, l]], ricci[[j, l]]}], {j, 1, n}, {l, 1, j}]

TableForm[Partition[DeleteCases[Flatten[listricci], Null], 2], TableSpacing → {2, 2}]

R[1, 1] $\frac{-f[r]\left(2f[r]+rf'[r]\right)g'[r]+rg[r]\left(f'[r]^2-2f[r]f''[r]\right)}{4rf[r]^2g[r]}$

R[2, 2] $-\frac{r\left(g[r]f'[r]+f[r]g'[r]\right)}{2f[r]}$

R[3, 3] $\frac{1}{4}\left(f'[r]g'[r]+g[r]\left(\frac{2f'[r]}{r}-\frac{f'[r]^2}{f[r]}+2f''[r]\right)\right)$

Calculating the scalar curvature:

The scalar curvature R is calculated using the inverse metric and the Ricci tensor. The result is displayed in the output line.

scalar = Simplify[Sum[inversemetric[[i, j]]ricci[[i, j]], {i, 1, n}, {j, 1, n}]]

$\frac{rg[r]f'[r]^2-2f[r]^2g'[r]-f[r]\left(rf'[r]g'[r]+2g[r]\left(f'[r]+rf''[r]\right)\right)}{2rf[r]^2}$

Calculating the Einstein tensor:

The Einstein tensor, $G_{\mu\nu}=R_{\mu\nu}-\frac{1}{2}g_{\mu\nu}R$, is found from the tensors already calculated.

einstein:=einstein = Simplify[ricci − (1/2)scalar ∗ metric]

The results are displayed in the same way as for the Ricci tensor earlier.

listeinstein:=Table[If[UnsameQ[einstein[[j, l]], 0], {ToString[G[j, l]], einstein[[j, l]]}],

{j, 1, n}, {l, 1, j}]

TableForm[Partition[DeleteCases[Flatten[listeinstein], Null], 2], TableSpacing → {2, 2}]

G[1, 1] $\frac{f'[r]}{2rf[r]}$

G[2, 2] $\frac{r^2\left(f[r]f'[r]g'[r]-g[r]\left(f'[r]^2-2f[r]f''[r]\right)\right)}{4f[r]^2}$

G[3, 3] $-\frac{f[r]g'[r]}{2r}$

Appendix C

Bibliography

[1] J. Voit, "One-dimensional Fermi liquids," Rep. Prog. Phys. **58** (1995) 977

[2] T. Giamarchi, "Quantum Physics in One Dimension," Oxford University Press, 2003

[3] H. J. Schulz, G. Cuniberti, P. Pieri "Fermi liquids and Luttinger liquids" [arXiv:cond-mat/9807366v2]

[4] M. Banados, C. Teitelboim and J. Zanelli, "The Black hole in three-dimensional space-time," Phys. Rev. Lett. **69** (1992) 1849 [hep-th/9204099].

[5] T. Faulkner, H. Liu, J. McGreevy and D. Vegh, "Emergent quantum criticality, Fermi surfaces, and AdS(2)," Phys. Rev. D **83**, 125002 (2011) [arXiv:0907.2694 [hep-th]].

[6] M. Kulaxizi and A. Parnachev, Nucl. Phys. B **815** (2009) 125 [arXiv:0811.2262 [hep-th]].

[7] V. G. M. Puletti, S. Nowling, L. Thorlacius and T. Zingg, JHEP **1201** (2012) 073 [arXiv:1110.4601 [hep-th]].

[8] F. Denef, S. A. Hartnoll and S. Sachdev, "Quantum oscillations and black hole ringing," Phys. Rev. D **80** (2009) 126016 [arXiv:0908.1788 [hep-th]].

[9] F. Denef, S. A. Hartnoll and S. Sachdev, "Black hole determinants and quasinormal modes," Class. Quant. Grav. **27** (2010) 125001 [arXiv:0908.2657 [hep-th]].

[10] D. Anninos, S. A. Hartnoll and N. Iqbal, "Holography and the Coleman-Mermin-Wagner theorem," Phys. Rev. D **82** (2010) 066008 [arXiv:1005.1973 [hep-th]].

[11] E. Witten, "Chiral Symmetry, the 1/n Expansion, and the SU(N) Thirring Model," Nucl. Phys. B **145** (1978) 110.

[12] L. D. Landau, "Theory of Fermi-liquids," Zh. Eksp. Teor. Fiz. 30 1058 (1956) Sov. Phys. JETP **3** 920 (1957)

[13] L. D. Landau, "Oscillations in a Fermi-liquid" Zh. Eksp. Teor. Fiz. 32 59 (1957) Sov. Phys. JETP **5** 101 (1957)

[14] L. D. Landau, "On the theory of the Fermi-liquid" Zh. Eksp. Teor. Fiz. 35 97 (1958) Sov. Phys. JETP **8** 70 (1959)

[15] R. Shankar, "Renormalization-group approach to interacting fermions," Rev. Mod. Phys. **66**, 129Ð192 (1994)

[16] J. Polchinski, "Effective field theory and the Fermi surface," In *Boulder 1992, Proceedings, Recent directions in particle theory* 235-274, and Calif. Univ. Santa Barbara - NSF-ITP-92-132 (92,rec.Nov.) 39 p. (220633) Texas Univ. Austin - UTTG-92-20 (92,rec.Nov.) 39 p [hep-th/9210046].

[17] B. Mihaila, "Lindhard function of a d-dimensional Fermi gas," [arXiv:1111.5337v1 [cond-mat.quant-gas]]

[18] A. M. Chang, "Chiral Luttinger liquids at the fractional quantum Hall edge," Rev. Mod. Phys. **75** (2003) 1449.

[19] J. W. G. Wilder, L. C. Venema, A. G. Rinzler, R. E. Smalley, C. Dekker, "Electronic structure of atomically resolved carbon nanotubes," Nature **391**, 59 (1998)

[20] D. C. Mattis and E. H. Lieb, "Exact solution of a many fermion system and its associated boson field," J. Math. Phys. **6** (1965) 304.

[21] J. S. Caux, "Abelian Bosonization Cookbook," Lecture notes of summer semester 2011 DITP course

[22] J. M. Maldacena, "The Large N limit of superconformal field theories and supergravity," Adv. Theor. Math. Phys. **2** (1998) 231 [Int. J. Theor. Phys. **38** (1999) 1113] [hep-th/9711200].

[23] S. S. Gubser, I. R. Klebanov and A. M. Polyakov, "Gauge theory correlators from noncritical string theory," Phys. Lett. B **428** (1998) 105 [hep-th/9802109].

[24] E. Witten, "Anti-de Sitter space and holography," Adv. Theor. Math. Phys. **2** (1998) 253 [hep-th/9802150].

[25] D. T. Son and A. O. Starinets, "Minkowski space correlators in AdS / CFT correspondence: Recipe and applications," JHEP **0209** (2002) 042 [hep-th/0205051].

[26] D. Birmingham, I. Sachs and S. N. Solodukhin, "Conformal field theory interpretation of black hole quasinormal modes," Phys. Rev. Lett. **88** (2002) 151301 [hep-th/0112055].

[27] J. McGreevy, "Holographic duality with a view toward many-body physics," Adv. High Energy Phys. **2010** (2010) 723105 [arXiv:0909.0518 [hep-th]].

[28] S. W. Hawking, "Black hole explosions," Nature **248** (1974) 30.

[29] E. Witten, "Anti-de Sitter space, thermal phase transition, and confinement in gauge theories," Adv. Theor. Math. Phys. **2** (1998) 505 [hep-th/9803131].

[30] S. A. Hartnoll and A. Tavanfar, "Electron stars for holographic metallic criticality," Phys. Rev. D **83** (2011) 046003 [arXiv:1008.2828 [hep-th]].

[31] P. Breitenlohner and D. Z. Freedman, "Stability in Gauged Extended Supergravity," Annals Phys. **144** (1982) 249.

[32] T. Faulkner, H. Liu and M. Rangamani, "Integrating out geometry: Holographic Wilsonian RG and the membrane paradigm," JHEP **1108** (2011) 051 [arXiv:1010.4036 [hep-th]].

[33] I. Heemskerk and J. Polchinski, "Holographic and Wilsonian Renormalization Groups," JHEP **1106** (2011) 031 [arXiv:1010.1264 [hep-th]].

[34] S. S. Gubser and I. Mitra, "Double trace operators and one loop vacuum energy in AdS / CFT," Phys. Rev. D **67** (2003) 064018 [hep-th/0210093].

[35] C. P. Herzog, P. Kovtun, S. Sachdev and D. T. Son, "Quantum critical transport, duality, and M-theory," Phys. Rev. D **75** (2007) 085020 [hep-th/0701036].

[36] S. A. Hartnoll, C. P. Herzog and G. T. Horowitz, "Building a Holographic Superconductor," Phys. Rev. Lett. **101** (2008) 031601 [arXiv:0803.3295 [hep-th]].

[37] S. A. Hartnoll, C. P. Herzog and G. T. Horowitz, "Holographic Superconductors," JHEP **0812** (2008) 015 [arXiv:0810.1563 [hep-th]].

[38] H. Liu, J. McGreevy and D. Vegh, "Non-Fermi liquids from holography," Phys. Rev. D **83** (2011) 065029 [arXiv:0903.2477 [hep-th]].

[39] M. Cubrovic, J. Zaanen and K. Schalm, "String Theory, Quantum Phase Transitions and the Emergent Fermi-Liquid," Science **325** (2009) 439 [arXiv:0904.1993 [hep-th]].

[40] J. Ren, "One-dimensional holographic superconductor from AdS_3/CFT_2 correspondence," JHEP **1011** (2010) 055 [arXiv:1008.3904 [hep-th]].

[41] T. Andrade, J. I. Jottar and R. G. Leigh, "Boundary Conditions and Unitarity: the Maxwell-Chern-Simons System in AdS_3/CFT_2," JHEP **1205** (2012) 071 [arXiv:1111.5054 [hep-th]].

[42] R. L. Arnowitt, S. Deser and C. W. Misner, "The Dynamics of general relativity," gr-qc/0405109.

[43] N. Iqbal, H. Liu and M. Mezei, "Quantum phase transitions in semi-local quantum liquids," arXiv:1108.0425 [hep-th].

[44] T. S. Bunch and L. Parker, "Feynman Propagator in Curved Space-Time: A Momentum Space Representation," Phys. Rev. D **20** (1979) 2499.

[45] F. Antonsen and K. Bormann, "Propagators in curved space," hep-th/9608141.

[46] T. Hartman and S. A. Hartnoll, "Cooper pairing near charged black holes," JHEP **1006** (2010) 005 [arXiv:1003.1918 [hep-th]].

[47] D. Vegh, "Holographic Fermi surfaces near quantum phase transitions," arXiv:1112.3318 [hep-th].

[48] A. Altland, B. Simons, "Condensed Matter Field Theory," Cambridge University Press, 2010